Vegetation Inventory of Legacy Seismic Lines in the Richardson Caribou Range

A report by the Alberta Biodiversity Monitoring Institute to the Forest Resource Improvement Association of Alberta for CHRP-21-04

November 2023

Executive Summary

Alberta's boreal woodland caribou (*Rangifer tarandus caribou*) are listed as Threatened by both the federal *Species at Risk Act* and, within Alberta, under the *Wildlife Act*. The Recovery Strategy for the Woodland Caribou Boreal Population outlines that caribou ranges must achieve and maintain a minimum of 65 per cent undisturbed habitat for populations to have a 60% likelihood of maintaining self-sustaining levels, where disturbance is classified as human footprint buffered by 500 m plus wildfires. The majority of ranges across Canada do not meet this target. As such, habitat restoration, particularly of legacy human footprint such as seismic lines, has been identified as an essential management action for caribou recovery. To facilitate operational planning for habitat restoration, there is an imminent need to develop vegetation inventories.

Following standards set out in the Government of Alberta's Provincial Restoration and Establishment Framework for Legacy Seismic Lines in Alberta (hereafter "the framework"), we have created a vegetation inventory on seismic lines in Alberta's Richardson caribou range (Version 1). The framework outlines the criteria that should be used to assess each seismic line to determine the most appropriate and optimal management interventions, if any, for each line. Using the framework's guiding principles, existing geospatial products as a foundation (e.g., existing Alberta Vegetation Inventory data, ABMI's Human Footprint Inventory and Wetland Inventory), and newly acquired aerial imagery, we categorized line segments into one of three actions as per the framework.

Key outcomes of this project are:

- A 26% increase in legacy seismic lines mapped in the range. Prior to this project, there were approximately 6,650 km of linear features mapped in the Richardson caribou range. Following our work, over 8,300 km of linear features were mapped, an increase of 1,669 km.
- We used alternative datasets such as SPOT imagery from the early 2000s to detect old seismic lines not visible in either aerial imagery or lidar, and manually added these regrowing lines to the dataset.
- We remapped seismic lines, creating an accurate understanding of length and area covered by linear features in the caribou range as well as a strong foundation for accurately tracking regeneration over time.
- The remapping of the seismic line footprint was completed using semi-automated methods. We continue to seek methods to speed up seismic line mapping for large areas. This is important for mapping new seismic lines and for establishing horizontally accurate locations that serve as a foundation for trend monitoring (e.g., how are seismic lines doing after management treatments).

- We provided high-quality vegetation structure metrics derived from lidar and validated by photo interpretation and field data. Lidar provides objective measures across wide areas, whereas interpreted values can be prone to interpreter bias. The systematic use of lidar means that any errors can be systematically reviewed and revised for all lines at once.
- Oblique photos and field data provide the “gold standard” for ground-truthing interpretation.
- Less than 1% of linear features are considered advanced regeneration using stereomodel interpretation. This value is greater when lidar canopy cover estimates are used, though the methods to arrive at the estimate differ from those of interpretation.
- We used lidar to establish canopy cover thresholds for different site types. Many site types naturally have under 70% canopy cover, suggesting that many lines may be further along the recovery trajectory than the 70% threshold and that vegetation characteristics in the surrounding forest should be considered.

Contents

Figures

portion on the left was sourced from FRIAA, while the portion on the right was flown by the ABMI.

Figure 13. Example of an area with an interpreted canopy cover value of 65% (of accepted tree species). Top left: aerial imagery. Top right: canopy height model layer. Bottom left: canopy cover estimate layer.

Figure 14. The relationship between interpreted cover of trees and shrubs with lidar-derived vegetation cover above 50 cm (Panel A) and lidar-derived canopy cover between 50 cm and 5 m in height (Panel B). Points are colored by interpreter. The dashed line represents a 1:1 relationship between the two measures of vegetation cover.

Figure 15. Site types and canopy cover estimates (CCE) for a portion of the Richardson caribou range where DEP data are available. The figure demonstrates how canopy cover thresholds vary between site types and are often below the 70% framework threshold.

Figure 16. Example of the value of site type-specific regeneration thresholds. The image on the left shows the abundance of lines classified as "treatment" (i.e., below a 70% canopy cover estimate) in the Richardson range. The image on the right shows only legacy seismic lines and trails with canopy cover greater than the average site type threshold derived from lidar. These lines may be further along the trajectory to recovery than a 70% threshold suggests.

Figure 17. Seismic lines and trails in the Richardson caribou range in the (left) Human Footprint Inventory 2021 and the Seismic Vegetation Inventory (SVI) dataset. The total length of seismic lines and trails is 6,659 km in HFI 2021 and 8,329 km in SVI.

Figure 18. Example of vegetation that would be recognizable in 15 cm aerial imagery.

Figure 19. Examples of 15 cm (top) and 30 cm (bottom) ground sampling distance (GSD) in an aerial photo compared to the field photo.

Figure 20. Example of pixel size at 15 cm (middle) and 30 cm (right) projected vertically at the black spruce sapling. The mass of vegetation large enough to be displayed at the minimum pixel size (15 cm, 30 cm respectively), indicated by the blue marker line, is offset from the measured height by approximately 30 cm (for GSD 15cm) and by 45 cm (for GSD 30 cm).

Tables

Table 1. Spatial accuracy statistics for the aerial triangulation block adjustments.

Table 2. Corresponding moisture regimes, Athabasca Plains Subregion ecosites, and Central Mixedwood Subregion ecosites for site type categories.

1. *Project rationale*

Landscape change resulting from human activities is a leading cause of changes in biodiversity worldwide (IPBES 2019; Miller-Rushing et al. 2019). Boreal woodland caribou (*Rangifer tarandus caribou*) in Alberta are listed as Threatened by both the federal *Species at Risk Act* and the provincial *Wildlife Act*. Features associated with the exploration for, and extraction of, resources have been linked to the decline of woodland caribou (Environment and Climate Change Canada 2020a; Hebblewhite 2017; Hervieux et al. 2013). In particular, linear features from energy exploration and extraction increase predator hunting efficiency and facilitate predator use of caribou habitat (DeMars & Boutin 2018; Dickie et al. 2017), resulting in increased caribou predation.

The federal recovery strategy for woodland caribou outlines that caribou ranges must achieve and maintain a minimum of 65 per cent undisturbed habitat for populations to have a 60 per cent likelihood of maintaining self-sustaining levels (Environment Canada 2012). The majority of ranges across Canada do not meet this target. As such, habitat restoration, particularly of legacy human footprint such as seismic lines, has been identified as an essential management action for boreal woodland caribou recovery (Environment and Climate Change Canada 2020b; Environment Canada 2012).

There is an imminent need for vegetation inventories to support operational planning for habitat restoration. The goal of this project funded by the Forest Resource Improvement Association of Alberta (FRIAA)—Vegetation Inventory of Legacy Seismic Lines in the Richardson Caribou Range—is to create a high-resolution vegetation inventory for linear features in the Richardson caribou range. The Richardson range covers 707,390 ha in northeastern Alberta, with anthropogenic footprint concentrated in the southern portion of the range (Figure 1).

This document describes:

- Methods used to collect and process aerial and ground-truthing data
- Methods used to create the vegetation inventory
- Engagement with Indigenous communities
- Overall range characteristics in terms of human footprint types, distribution, and level of natural regeneration
- Attributes associated with linear features in the geodatabase

The outcomes from this project will ultimately support efforts to sustain and improve caribou habitat in a manner that supports healthy and self-sustaining caribou populations.

Figure 1 . Overview map of the Richardson caribou range in northeastern Alberta and human footprint from the ABMI Human Footprint Inventory 2021.

2. Ground-truthing data collection

A two-part field verification program supported the remotely sensed components of the vegetation inventory.

a. Field validation

Field campaigns occurred in fall 2021 and summer 2022 to collect imagery, video footage, and vegetation data for both interpretation training and quality assurance. A total of 84 sites in six focal areas were visited during the field campaigns (Figure 2).

The field campaign in fall 2021 collected information to support imagery interpretation. Field crews visited two focal areas (with a minimum of 15 photo locations per focal area) in the Richardson range. Photo locations were a mixture of low impact and legacy seismic lines with differing orientations (e.g., N-S or E-W), in areas with differing linear feature density, burns, and site types (upland/wetland). Each photo location targeted vegetation types capable of growing over 5 m in height.

At each location, crews collected either:

- A 360° photo taken from a tripod at a height of 1.5 m; photo includes 2 m reference pole adjacent to vegetation for height estimation; or
- Five representative photos, showing "up" and "down" the line (e.g., one photo north and one photo south if line runs N-S), a photo of each side (e.g., the east and west sides of a N-S line), and a photo pointed directly down at the ground, with the 2 m reference pole.

Other data collected at each point include:

- Line width
- Line orientation
- Tree and shrub species present (within 5 m of photo location), including species that will not grow to 5 m
- Density and height categories of each species capable of growing above 5 m in height
- Dominant species (maximum of 5) in the top layer of vegetation
- Video footage collected while traveling between photo locations within the focal area using a GoPro camera

The field campaign in summer 2022 collected information for interpretation validation using the collaboratively developed Boreal Ecosystem and Recovery Assessment (BERA) *Field Protocol for Helicopter Access* to maximize the utility of the collected data. Crews visited sites in four focal areas. At each site, crews collected information including:

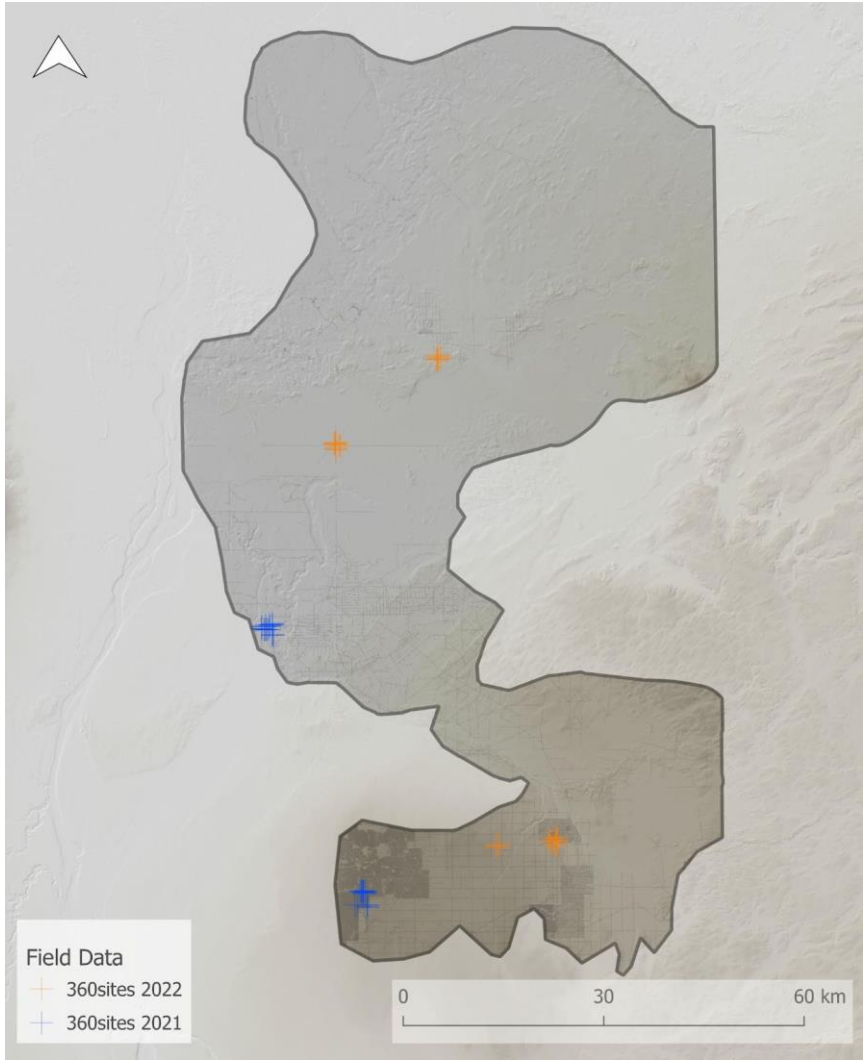

Figure 2. Locations of ground-truthing sites visited in 2021 and 2022.

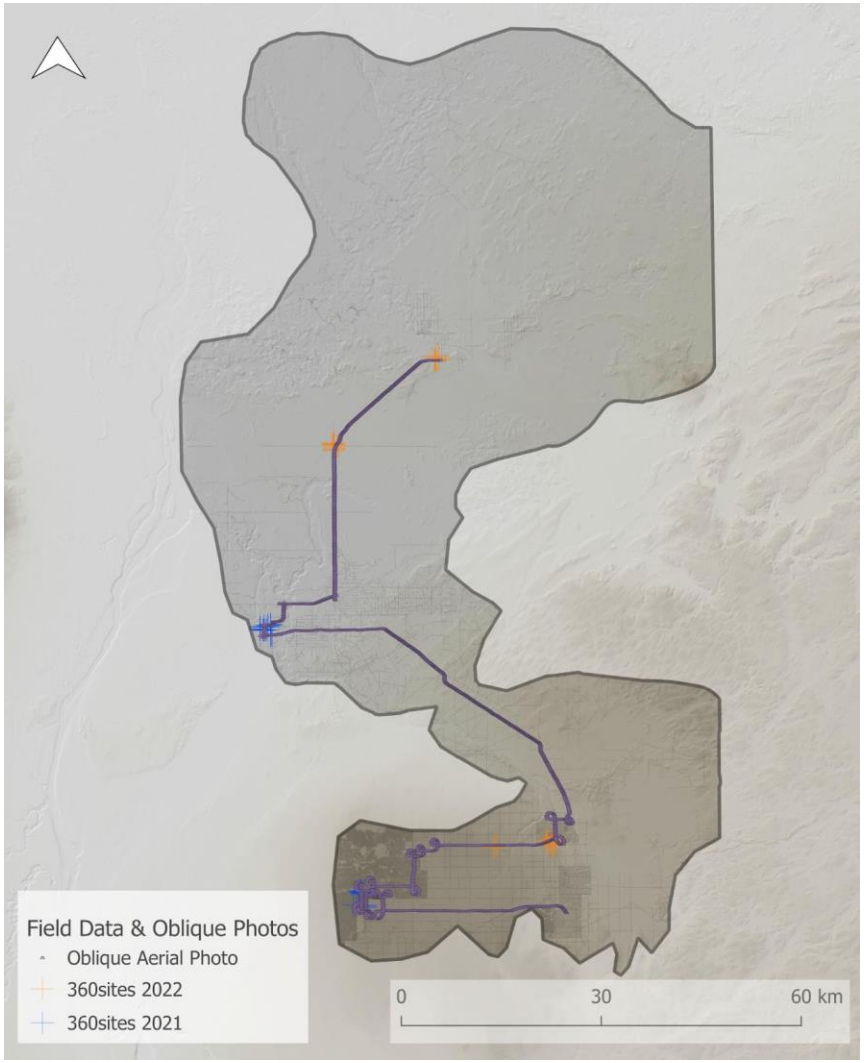

Figure 3. Flight path for oblique imagery collection. Imagery was collected in August 2022 and targeted areas where ground-truthing field sites were located.

- Line width
- Line orientation
- Line treatment status (treated or natural)
- Ecosite and site type
- Five representative photos, showing “up” and “down” the line (e.g., one photo north and one photo south if line runs N-S), a photo of each side (e.g., the east and west sides of a N-S line), and a photo pointed directly down at the ground.
- Presence of vehicle or wildlife trails, soil compaction, restoration treatment type, wet soils, and non-tree competition
- Cover, height, and/or tree counts for vegetation layers

b. *High-resolution oblique imagery*

Oblique imagery was collected along a 200 km flight path via fixed wing aircraft in August 2022. This imagery was used for interpretation calibration and to validate interpretation in the final geospatial dataset. The flight path is shown in Figure 3; it was designed to capture imagery for areas where ground-truthing field data was also collected, creating “gold standard” verification datasets. An example of oblique imagery is shown in Appendix 2.

3. *Vegetation inventory methodology*

a. *Aerial data collection*

Imagery was collected by Peregrine Aerial Surveys Inc. (PASI) using a high-end, large-frame aerial digital camera sensor, DMC III, mounted in a Piper PA31 (Navajo) plane. Aerial photos were captured using five cameras, each for a separate spectral band (Panchromatic, Red, Green, Blue, and Near-Infrared). The spatial resolution of the image acquisition was under 15 cm to ensure that the resulting ground sampling distance (GSD) of the orthophoto mosaic created by resampling was 15 cm. Images were captured with 80% forward overlap and 40% sidelap overlap. Average flight altitude was 3,700 meters above mean sea level. Imagery was acquired on October 3, 7, and 8, 2021, during leaf-on conditions in the southern portion of the range. The color of leaves for deciduous species was changing from a green color scale to a yellow/brown color scale during this period, supporting photo

interpretation for tamarack as well as deciduous trees and shrubs. The imagery collected in fall 2021 was triangulated in three blocks (Block 1, Block 2, Block 3) (Figure 4).

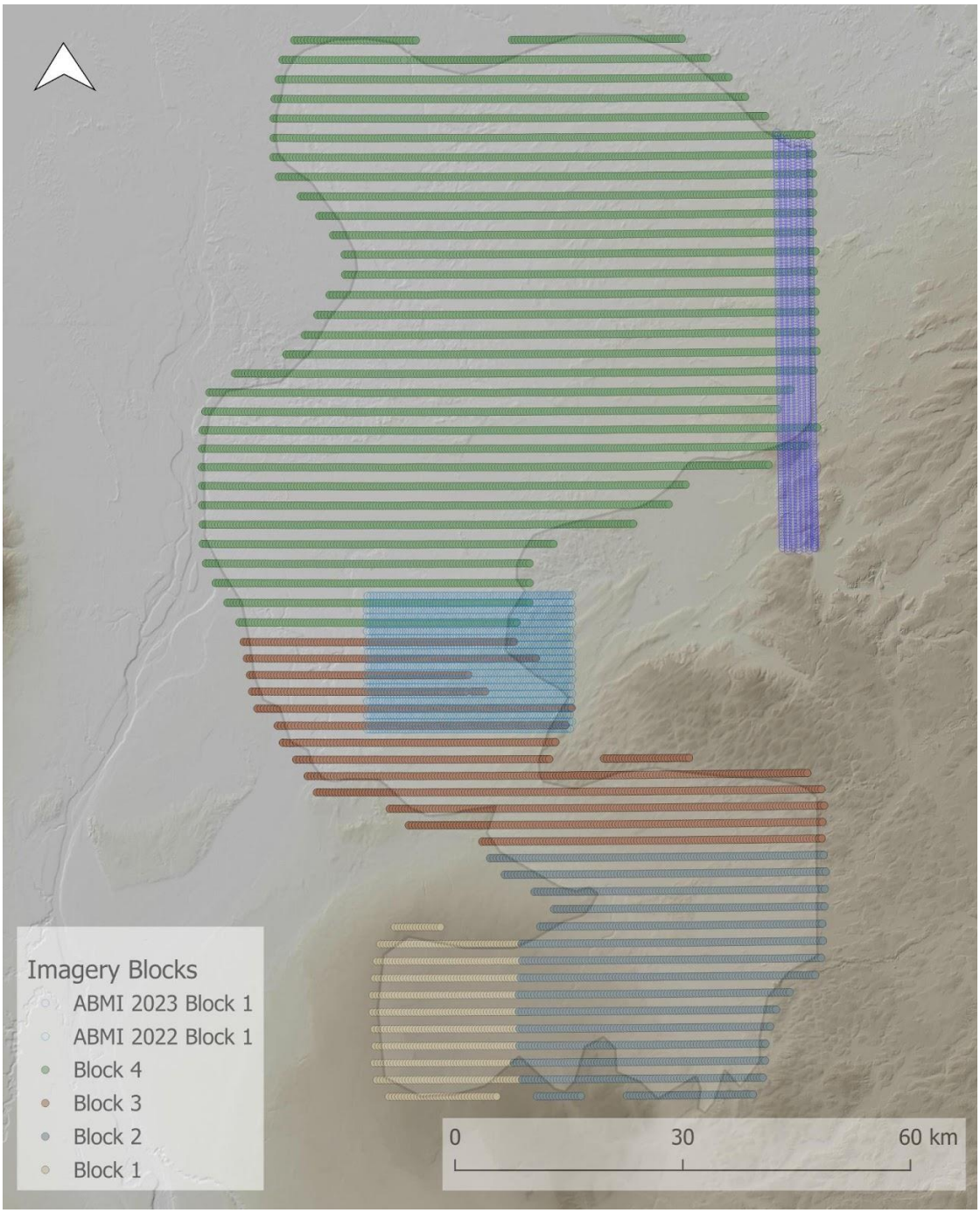

Figure 4. Aerial triangulation blocks for the Richardson caribou range.

The majority of seismic lines are narrow corridors within taller vegetation. Increased sidelap overlap captures seismic lines that are parallel to the flight direction closer to the nadir position of the aerial photograph, giving interpreters a less obstructed view of the ground area on the seismic line.

A second period of imagery collection in the northern portion of the range took place in fall 2022. Imagery was acquired on September 5 and September 30, 2022, with the same specifications and equipment as imagery in 2021. After the imagery collected in 2022 was received, we verified the number of bands, image resolution, imagery extent, and whether a stereo model set-up was provided for raw imagery. During routine checks, it was determined a small portion of the imagery collected in 2022 was corrupted due to equipment failure. There was also a reduced quality of imagery due to environmental conditions (smoke) during the acquisition period on a smaller portion of the project area. The reduced quality of the imagery did not affect our ability to interpret imagery as only the color of the imagery was modified, not the spatial resolution. We compensated by stretching the histograms of the imagery within the softcopy environment during data capture. Using 1.5 m resolution SPOT satellite imagery, we determined that the corrupted area did not contain any seismic lines. The imagery collected in fall 2022 was triangulated within one block (Block 4) (Figure 4).

Additional aerial imagery covering the corrupted area in the northeastern portion of the range was acquired on July 4, 2023, by the ABMI. We used a high-end aerial camera, Phase One iXM-RS150F, with focal length of lens configuration 70 mm. The spatial resolution of the aerial imagery acquired by ABMI's camera ensured a GSD of 11 cm. Summer 2023 imagery was reviewed and it was confirmed that there are no seismic lines within the area. The imagery collected in the summer 2023 was triangulated in one block (ABMI 2023 Block 1) (Figure 4).

The ABMI had also acquired high-resolution aerial imagery in the central portion of the range on August 12, 2022, to supplement existing aerial coverage. We used a high-end aerial camera, Phase One iXM-RS150F, with focal length of lens configuration 70 mm. The spatial resolution of the aerial imagery acquired by ABMI's camera ensured a GSD of 11 cm. The imagery collected in summer 2022 was triangulated in one block (ABMI 2022 Block 1) (Figure 4).

b. Aerial data processing

We generated stereomodels and high-resolution multiband orthophoto mosaics from the aerial imagery through the following steps:

Aerial triangulation – Aerial imagery was organized into blocks based on the direct georeferencing information (Figure 4). We adjusted each block using an aerial triangulation bundle adjustment process to identify the position of photo centers and orientation of the camera at the moment of exposure. The accuracy of each block adjustment was determined by comparing randomly distributed elevation points with a bare earth elevation model. Ten checkpoints randomly distributed over the project area within Block 1 were used to confirm vertical accuracy. The root square error of Z coordinates (RMSz) of check points within Block 1 was 0.35 m. The spatial accuracy statistics (mean, RMS, maximum and number of observations) of the aerial triangulation block adjustments are displayed in Table 1.

Table 1. Spatial accuracy statistics for the aerial triangulation block adjustments.

		X	Y	Z	Exy
Block 1	mean absolute	0.121	0.103	0.084	0.175
	RMS	0.153	0.128	0.114	0.199
	maximum	0.548	0.388	0.432	0.579
	number of frames	501	501	501	501
Block 2	mean absolute	0.102	0.136	0.053	0.188
	RMS	0.127	0.172	0.068	0.214
	maximum	0.433	1.03	0.244	1.032
	number of frames	1336	1336	1336	1336
Block 3	mean absolute	0.100	0.128	0.059	0.178
	RMS	0.124	0.157	0.077	0.200
	maximum	0.425	0.63	0.327	0.679
	number of frames	1449	1449	1449	1449
Block 4	mean absolute	0.102	0.123	0.051	0.176
	RMS	0.129	0.152	0.066	0.199
	maximum	0.723	0.639	0.272	0.724
	number of frames	4805	4805	4805	4805
Block ABMI camera	mean absolute	0.114	0.147	0.158	0.206
	RMS	0.144	0.186	0.194	0.235
	maximum	0.61	0.663	0.644	0.692
	number of frames	1418	1418	1418	1418

Orthorectification – Orthorectification is the process of creating a constant scale across aerial photos, as aerial imagery is distorted by the tilt of the camera, the camera distortions, and elevation changes in terrain. We used a digital terrain model (DTM) to create a seamless bare earth mosaic of elevation raster. This file was used as a base for the orthorectification process. The orthorectification process generated one orthophoto per aerial image with a spatial resolution of 15 cm (meeting targets outlined in Section 7.3.2 of the provincial restoration framework).

Digital surface model generation – A digital surface model dataset was generated by high-end photogrammetric software, using the Semi-Global Matching method. The digital surface models were used to create canopy height model (CHM) raster datasets by subtracting values of topographic elevations stored in bare earth elevation rasters. Canopy height models were created from aerial imagery frames once aerial imagery blocks were adjusted (Figure 5). The spatial resolution of resulting CHMs was 15 cm.

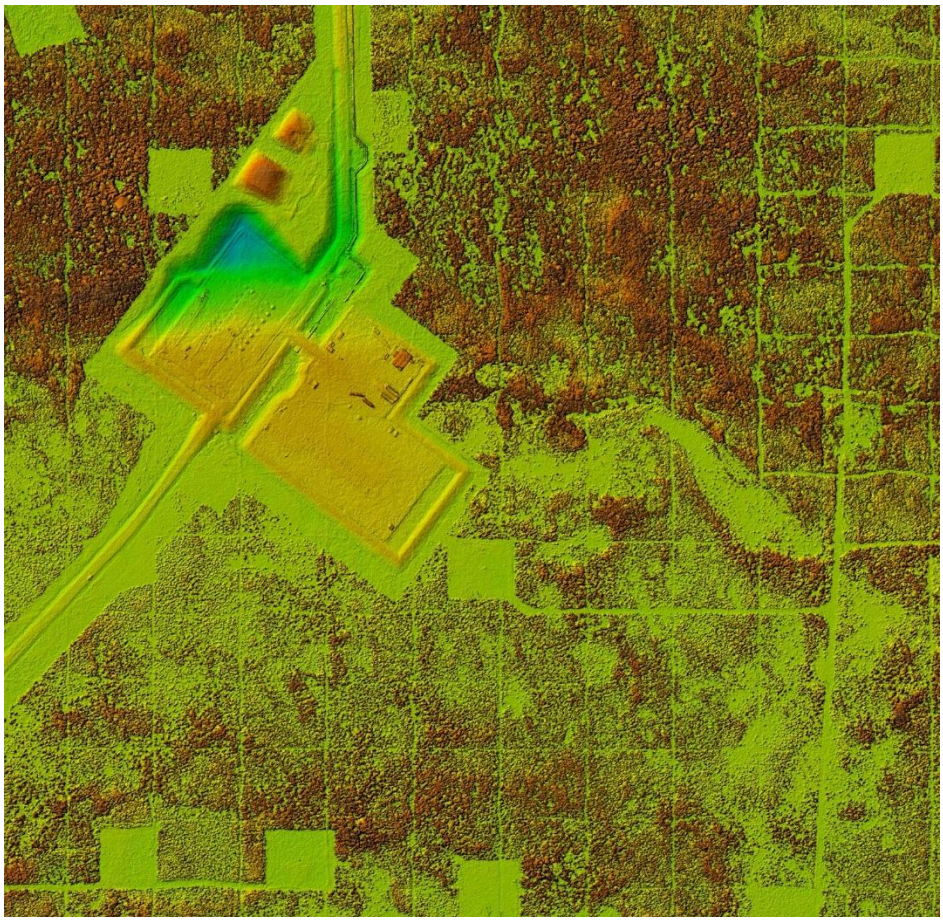

Figure 5. Example of a canopy height model for a portion of the Richardson caribou range. The colour gradient (from green to red) indicates the height of the point above the surface, light green representing the surface or lowest points.

c. *Human footprint correction*

Confirming the exact distribution and location of human footprint is critical to accurately track vegetation regrowth and the state of caribou habitat. Missing features result in an underestimation of both the extent of habitat modification and potentially the extent and regrowth. Uncorrected features will perpetuate errors in geospatial analyses through a misalignment between the feature's footprint and vegetation layers (e.g., adjacent vegetation may be included in analyses).

The latest version of the ABMI's Human Footprint Inventory (HFI) dataset available at the time of project onset—the 2019 version—was used as a basis for this project. The HFI is created through heads-up digitization of satellite scene mosaics with a spatial resolution of 1.5 m. The entire area of the province is reviewed by trained interpreters at a 1:30,000 scale and all new digitization is performed at a scale of 1:5,000. The HFI dataset is sufficient for reporting on human footprint, however, its spatial accuracy and generalization of the digitized features is not sufficient for inventorying vegetation on seismic lines as even small misplacements (due to generalization and horizontal accuracy) would limit the ability to interpret the vegetation on the narrow corridors of linear features.

New centerlines of each seismic line and trail were created by either a semi-automated approach using the Forest Line Mapper tool or digitization of the new line by trained interpreters within high-resolution 3D stereomodels (Figure 6). Forest Line Mapper (FLM) is software created by the Boreal Ecosystem Recovery and Assessment (BERA) project at the University of Calgary (Applied Geospatial Research Group 2021). It facilitates high-resolution mapping of linear features by processing canopy height models and other data to determine the "path of least resistance" and thus delineate lines in forested areas.

The inventory's features were reviewed by interpreters in 3D environments of high-resolution aerial stereomodels, allowing edits previously not possible when human footprint digitization decisions were made only on lower resolution 2D imagery products (i.e., a SPOT satellite scene mosaic).

There were two major differences between the current HFI and the updated Seismic Vegetation Inventory (SVI) dataset.

First, we removed trails from the HFI when there was no evidence the features existed on the landscape. These features were most likely previously digitized based on SPOT satellite scenes (lower resolution imagery) following temporary (i.e., not permanent) land cover modifications. Most removals were applied in the north part of the project area. An example of trail features removed from the HFI is shown in Figure 7 in a yellow ellipse; the total length of the removed trails is approximately 390 km.

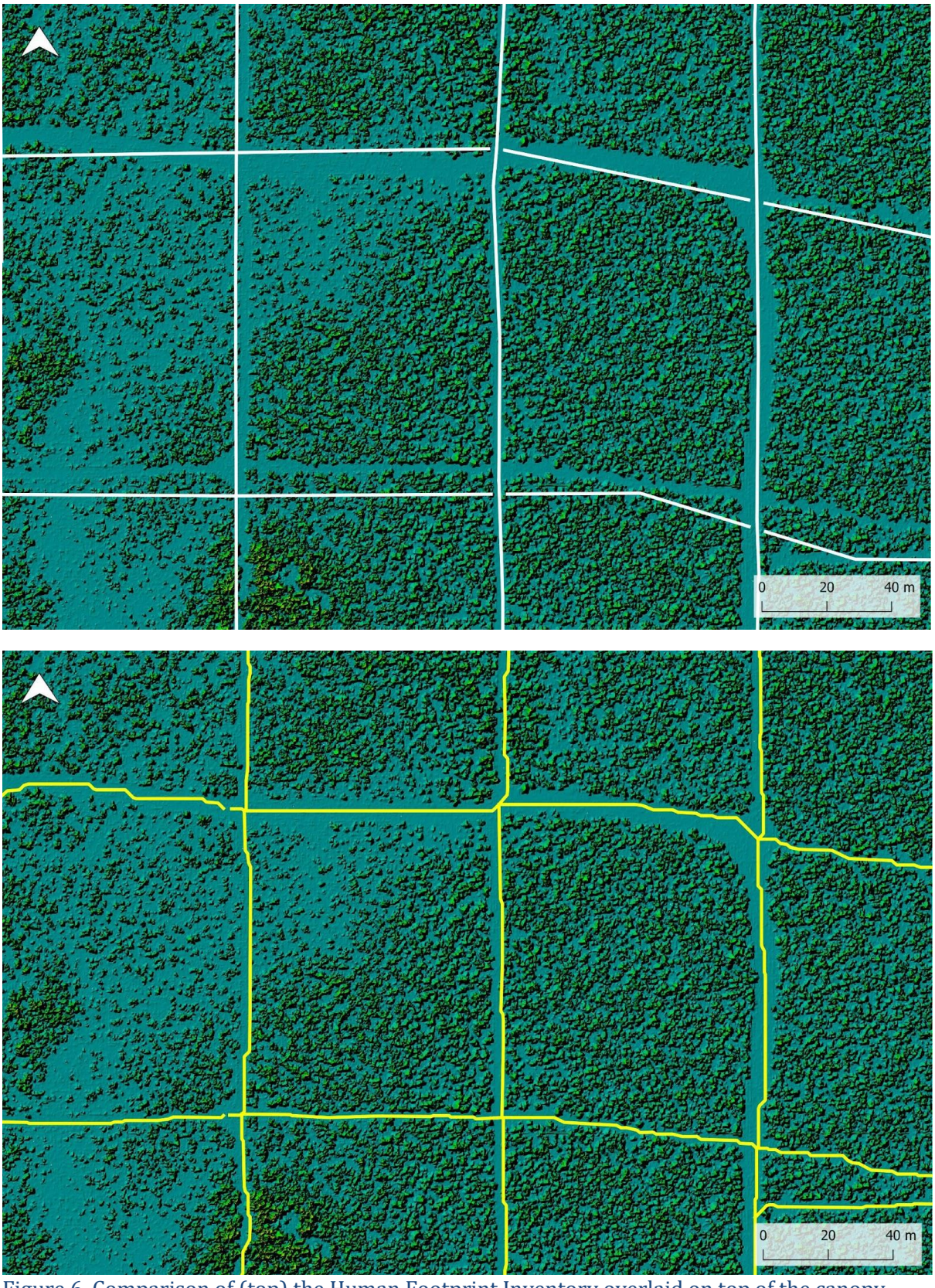

Figure 6. Comparison of (top) the Human Footprint Inventory overlaid on top of the canopy height model and (right) the SVI dataset overlaid on top of the canopy height model. Correcting centrelines is a critical step in understanding and tracking the state of vegetation regrowth.

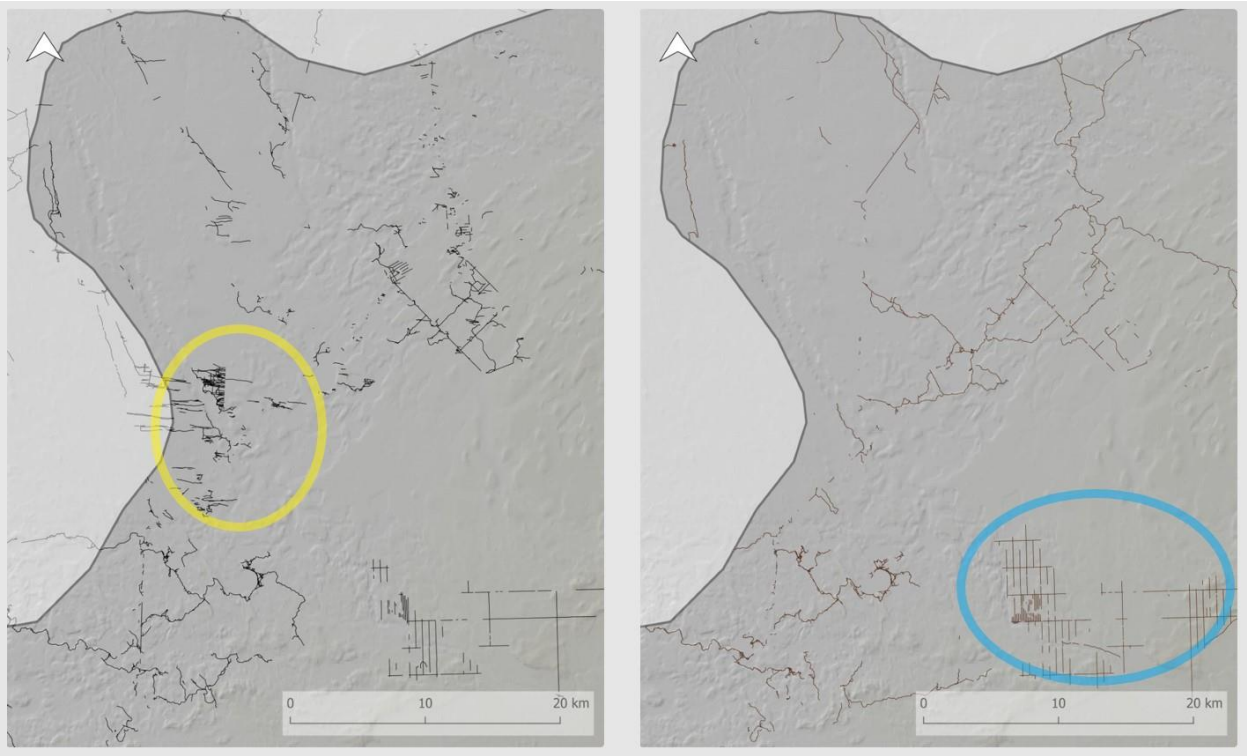

Figure 7. Comparison of the Human Footprint Inventory and the updated human footprint dataset used for the vegetation inventory, termed the Seismic Vegetation Inventory dataset. The yellow ellipse shows an example of trails removed due to a lack of physical evidence for their existence in imagery. The blue ellipse shows an example of linear features added to the SVI dataset after reviewing aerial and historical datasets.

The second, more common update was adding linear features (trails, legacy seismic lines, or low impact seismic lines) where such features were not present in the HFI but there was clear evidence in 3D stereomodels of their presence on the landscape. Figure 7 shows an example of seismic line features added to the HFI in a blue ellipse. Historical reference datasets were also reviewed to provide information about the existence of seismic lines that might not be visible on the current stereo models; these features would have been overlooked if historical datasets were not used. The orthophoto grayscale mosaic created by the ABMI from aerial photos acquired by the Government of Alberta (GoA) for 1980 base mapping was used as a main historical reference imagery dataset (Figure 8). The spatial resolution of 1980s orthophoto mosaics is 1.25 m. The grayscale mosaic of SPOT 2005 satellite scenes with a spatial resolution 2.5 m, provided by the GoA, was also used.

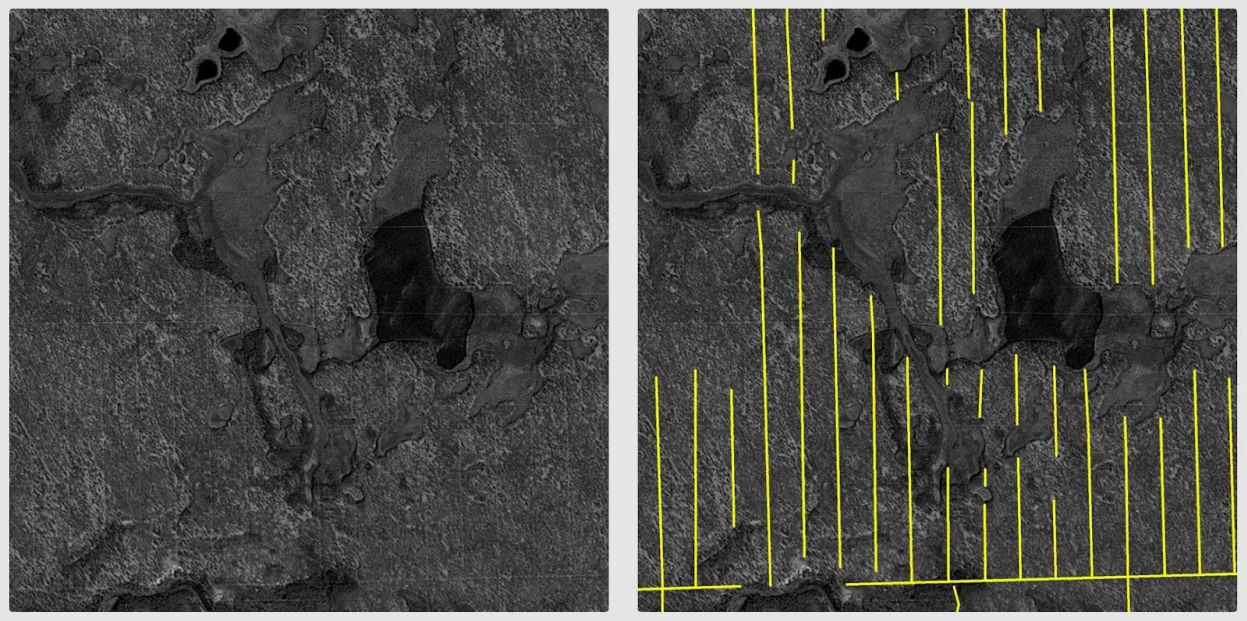

Figure 8. Example of orthophotos from 1980 used as a historical reference dataset. The image on the right highlights the seismic lines added through detailed review of alternative datasets.

Despite the extensive review process, there is a possibility that some old seismic lines are not included in the dataset if there was no clear evidence in either the current aerial stereomodels or the historical orthophotos. We hope our next version of caribou habitat mapping that includes full coverage of lidar data will help identify such "hidden" features.

This review of the HFI was a critical step to turn a planning inventory into an operational dataset. While the HFI's horizontal accuracy requirements are sufficient for reporting on human footprint at larger scales, missing features and even small misalignments with the actual linear corridor can lead to misinterpreted values about the status of vegetation and inhibit tracking recovery over time using remote sensing. It is crucial to verify both the full extent of linear features and their exact position on the landscape prior to operationalizing restoration.

d. Seismic line alignment

In the FLM process, the HFI was used as a reference source to help identify existing linear features (seismic lines and trails). The entire processed area was reviewed by an interpreter trained on human footprint and manual edits were applied when needed. These manual edits consisted primarily of moving the start and end points of a line into the centre of the corridor to fix the position of the first and the last point of the line. The FLM process

used canopy height models to calculate the new centralized position of all inner vertices of the line feature (Figure 9).

Not all lines were created by the semi-automated FLM process. The FLM process requires manual interaction, line input preparation and line output quality control; this process was therefore time-consuming and efficient only in areas where the density of linear features was very high, typically in areas of dense low impact seismic line grids. We chose different approaches in areas where the density of linear features was low and where manual digitization of lines in the stereomodel by an experienced interpreter was faster and more

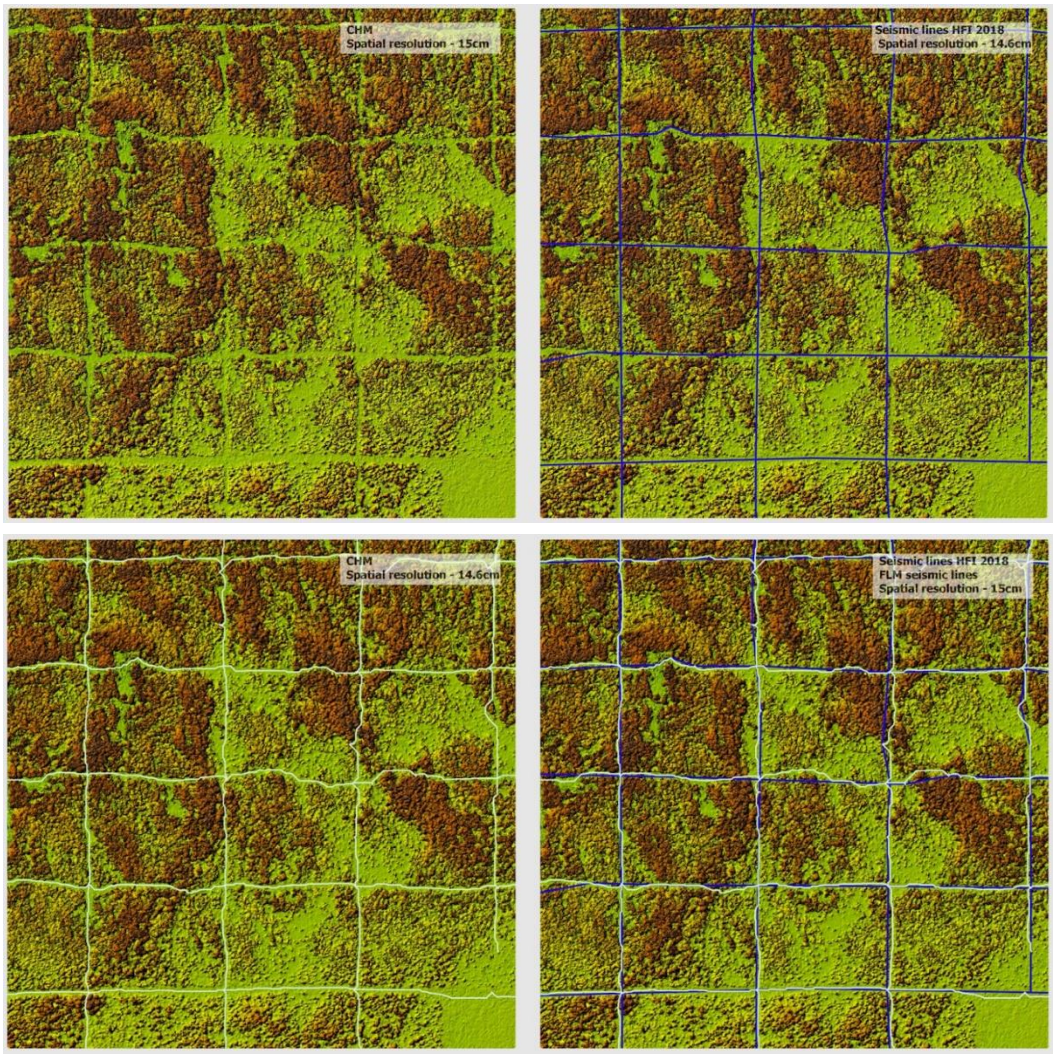

Figure 9. Example of Forest Line Mapper (FLM) process. Top left: canopy height model. Top right: seismic lines from the Human Footprint Inventory 2018 prepared for FLM processing. Bottom left: seismic lines generated by the FLM process. Bottom right: Both HFI and FLM seismic lines overlaid on the canopy height model.

efficient, typically in areas with a lower density of legacy seismic lines and trails (see ABMI 2019 for a guide to human footprint interpretation).

One of the attributes created during the FLM process was "average width of the linear corridor." This attribute is included in the final attributes of the SVI dataset.

e. Imagery interpretation

Imagery interpretation was conducted by experienced photo interpreters. All line segments were classified by site type, line width, and line orientation, and categorized as treatment, exclusion, or advanced regeneration. Site type categories (Upland Dry, Upland and Transitional, Lowland Treed, or Lowland Low Density Treed) were either interpreted or, on locations where line segments were overlaid by existing ecosite inventory polygons, derived from the Derived Ecosite Phase (DEP) and Primary Land and Vegetation Index (PLVI) inventories, based on ecosite and depending on natural subregion (Table 2). There are three natural subregions within the Richardson caribou range boundary: Athabasca Plain, Central Mixedwood, and Kazan Uplands (Figure 10). There are no seismic lines or trails in the area of Kazan Uplands. The ecosite information from the inventories was transferred into the Seismic Vegetation Inventory in the form of an attribute for each line segment (Figure 10, Figure 11).

Table 2. Corresponding moisture regimes, Athabasca Plains Subregion ecosites, and Central Mixedwood Subregion ecosites for site type categories.

Site Type	Corresponding Moisture Regime	Corresponding Athabasca Plain Ecosite	Corresponding Central Mixedwood Ecosite
Upland Dry	Xeric, Subxeric, Submesic, Mesic	a1, b1, c1, c2, d1, d2, d3, d4, d5, d6, e1, f1, f2, f3, f4, f5	a1, aa1, aa2, b1, b2, b3, b4, b5, b6, b7, c1, c2, d1, d2, d3, d4, d5, d6, e1, e2, e3, e4, e5
Upland and Transitional	Subhygric, Hygric, Subhydric	g1, g2, g3, g4, g5, h1	f1, f2, f3, f4, f5, g1, g2, h1, h2, h3
Lowland Treed	Subhydric, Hydric	i1, j1, k1	i1, j1, k1
Lowland Low Density Treed	Subhydric, Hydric	i2, i3, j2, j3, k2, k3, l1	i2, i3, j2, j3, k2, k3, l1

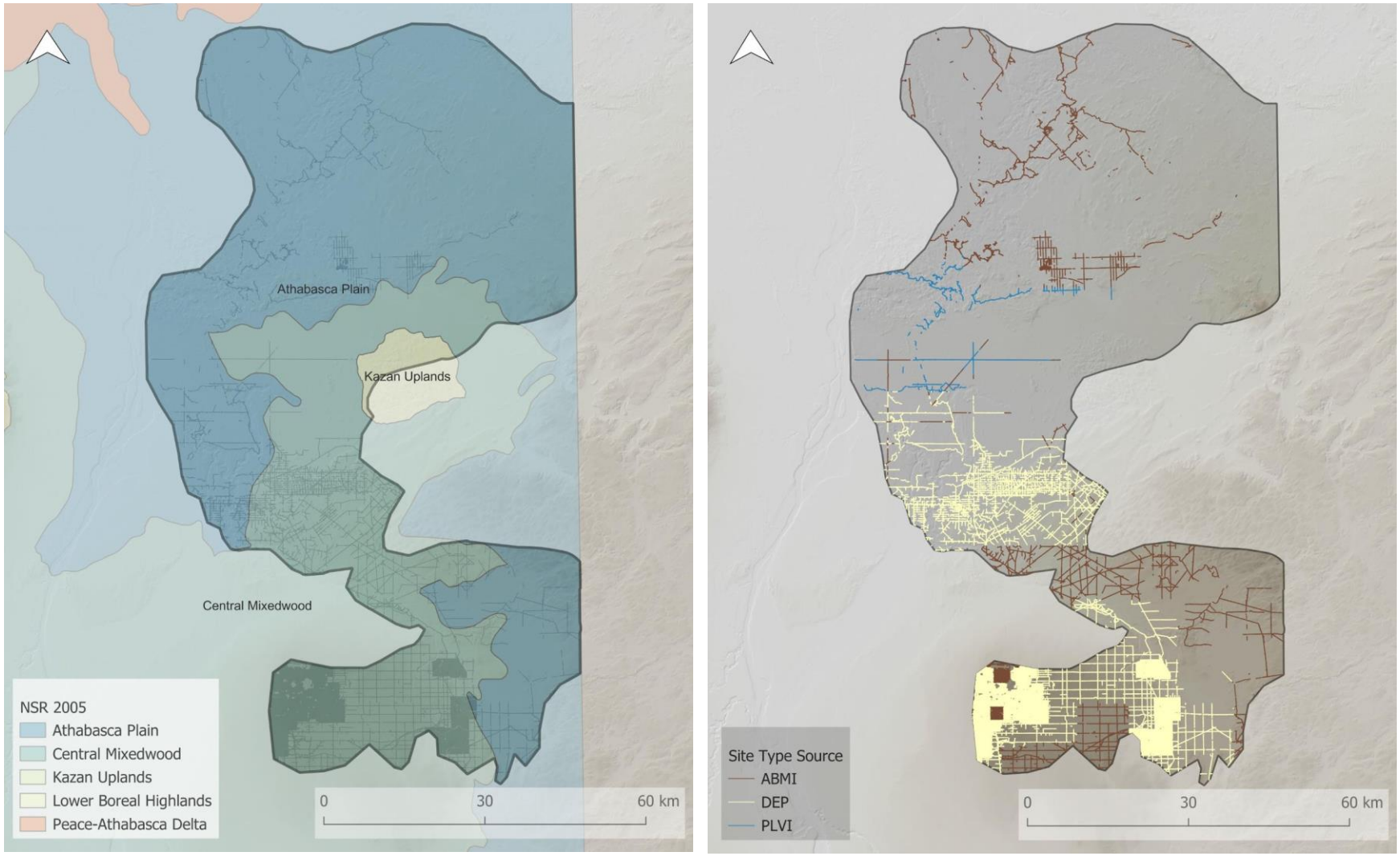

Figure 10. Natural subregions of Alberta in the Richardson caribou range and the data source for site types. Features in brown were classified by ABMI interpreters. Features in yellow were associated with Derived Ecosite Phase (DEP) polygons, while features in blue were associated with Primary Land and Vegetation Index (PLVI) polygons.

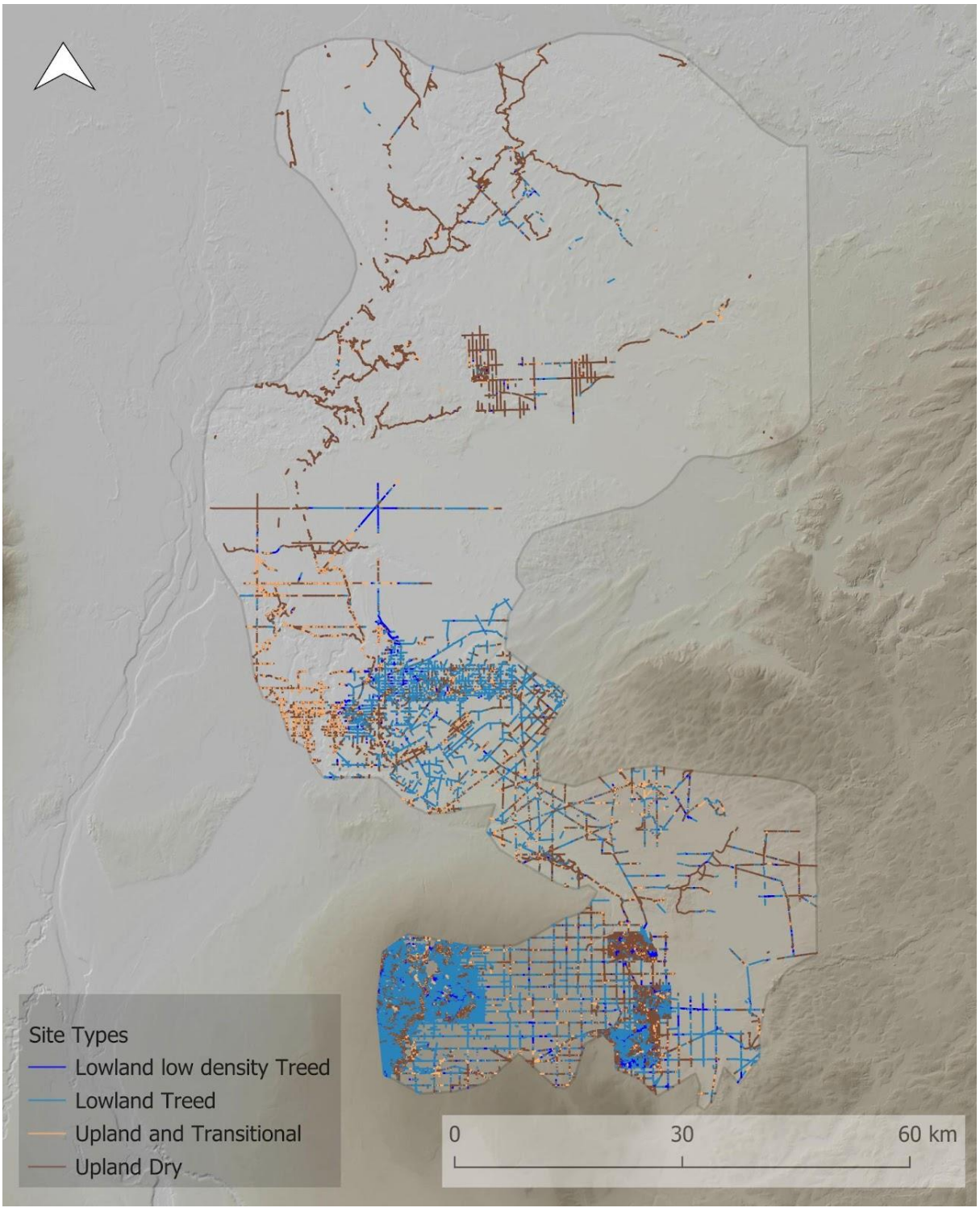

Figure 11. Site types on linear features and trails in the Richardson range.

The Government of Alberta has developed the Provincial Restoration and Establishment Framework for Legacy Seismic Lines in Alberta (Government of Alberta, 2018; hereafter the "framework"). The framework outlines the criteria that should be used to determine the most appropriate management interventions, if any, for each seismic line. Our inventory includes categorizations for each linear segment for one of three framework actions: Treatment, Advanced regeneration, and Exclusion.

- **Treatment**: Areas that do not show existing advanced regeneration and are thus candidates for restoration treatments.
- **Advanced regeneration**: Areas that are regenerating naturally and do not require treatment. We used Section 3.3, Section 5.5, and Table 4 from the framework to classify natural regeneration. Specifically, we evaluated if the segment has >70% coverage of species that are capable of reaching a height of 5 m with no less than 50% coverage on either side of the line. We also noted the presence of human access and wildlife trails to facilitate the planning of treatments such as tree felling or coarse woody debris placement to limit predator or human access. We are able to confidently interpret the species, density, and height of coniferous and deciduous trees, as well as the height and density of shrubs.
- **Exclusion**: Areas that are not treed or are considered outside the framework, including riparian areas, outwash plains, grassy montane areas, open fens, etc.

Segments identified as "exclusion" were removed from further vegetation interpretation. The remaining segments were classified as "treatment" or "advanced regeneration" based on the percent coverage of species capable of reaching a height of 5 m, and the presence or absence of human access trails.

If estimated canopy coverage was greater than 70%, interpretation continued to evaluate the composition of the treed vegetation for the presence or absence of tree species that are on the approved list in the framework. Line segments were classified as "advanced regeneration" if the canopy cover estimate was greater than 70% for approved tree species only: for example, shrubs or trees present on the line segment but not on the approved tree species list (e.g., willows, birch, Labrador tea) were ignored. Up to three tree species were interpreted for each line segment of advanced vegetation along with their average height. If vegetation cover of approved tree species was less than 70%, the line segment was classified as "treatment", and no further information was interpreted.

The canopy cover of naturally regenerating vegetation is a non-linear, complex temporal process depending on many factors (e.g., tree species, competition, landscape conditions, microclimate). A single threshold value might not optimally represent the best approach to evaluate the ongoing process of vegetation regeneration, therefore the manually interpreted values were supplemented by values derived from an additional dataset: lidar.

The lidar dataset covered a subset of the entire project area; lidar acquisition planned to cover the entire province of Alberta was not completed at the time of the project, but will be available for future vegetation inventory work. However, a significant portion of legacy seismic lines and trails (77%) were covered with the high density (16 pts/m^2) lidar point clouds, which allowed the creation of enhanced vegetation measurements using derived lidar products for a large subset of the features of interest.

f. Lidar data collection

The lidar data used in developing enhanced vegetation metrics was sourced from both FRIAA and the ABMI. Lidar data was collected for the region in July to September 2022 by the ABMI; the data from FRIAA was flown June to August 2022 (Figure 12). In total, lidar coverage was available for 272,412 ha, representing 38.5% of the Richardson range.

The ABMI's data acquisition flights used a Piper Navajo PA31-310 aircraft. Lidar was acquired by a high-end aerial lidar sensor (Galaxy T2000), at an average altitude of 2,000 m above terrain. Scan angle of the lidar sensor was set 25 degrees from the nadir position. The average speed of the flight was 75 m/second.

For the lidar collected by the ABMI, raw lidar data were extracted, and block adjustment was performed to produce a geometrically accurate point cloud dataset in standardized file format (.las). This process was broken down into two steps termed 1) Lidar Mapping Suite (LMS) and 2) LAStools (rapidlasso 2022) for data calibration and classification.

The LMS process decoded the raw sensor files and created lidar point clouds in the standardized file format (.las). The LMS process consisted of a series of steps to calculate GPS trajectories, remove systematic errors based on boresight calibration values, remove noise, and correct flight line inaccuracies. The height difference between flight lines was calculated during the LMS process. The average vertical difference between the flight lines was 0.0558 m and standard deviation of the vertical differences between the flight lines was 0.0052 m.

In LAStools, LAS files were subsequently indexed, cleaned to remove any remaining noise, and categorized to two classes: ground and unclassified. The ground points represent the locations of the lidar returns assumed to be on the bare earth - ground without any vegetation or structure above the ground. All other points—including lidar returns from vegetation, structures above the ground, and remaining noise points—were placed into the "unclassified" category.

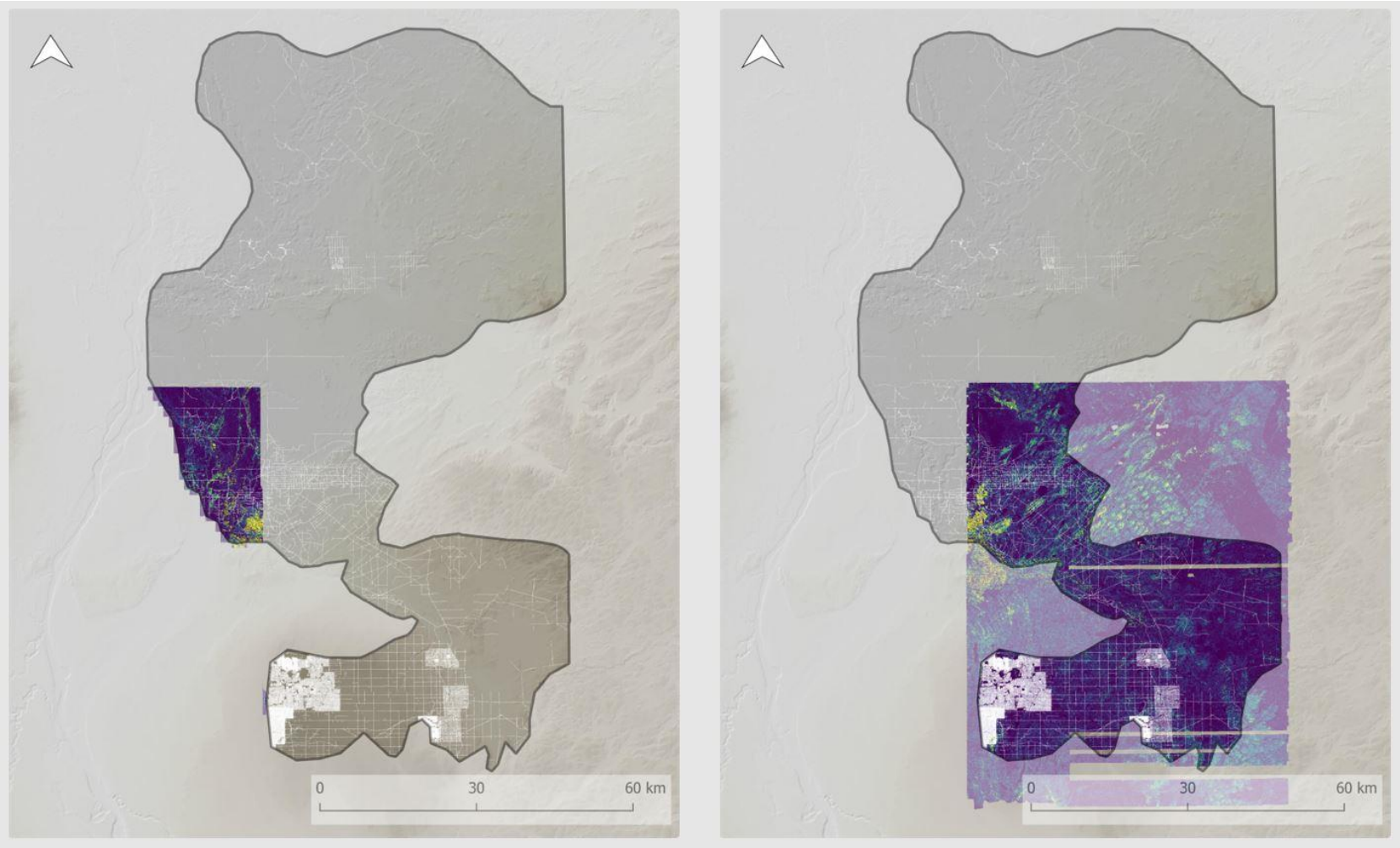

Figure 12. Lidar coverage of the Richardson range, displayed as a canopy height model (CHM), covering an area containing 77.28% of the legacy seismic lines and trails. The portion on the left was sourced from FRIAA, while the portion on the right was flown by the ABMI.

a. Lidar quality control and processing

Quality control was preformed for both previously acquired (external; FRIAA) and newly collected (ABMI) data to ensure datasets met industry standards defined by the American Society for Photogrammetry and Remote Sensing (ASPRS).

For the external lidar data, 10% of the tiles were randomly selected and manually reviewed to determine density and spacing of the lidar point clouds within inspected tiles. Classification and presence of noise in the dataset was also confirmed.

For ABMI-collected lidar data, we developed and implemented a QC process to ensure standardized data quality. There were 291 Non-vegetated Vertical Accuracy (NVA) checkpoints distributed over the area of the ABMI lidar block. The ABMI lidar block consists of three processing subblocks, calculated separately. The NVA checkpoints were not ground surveyed, but they were derived from lidar provided to the ABMI by the Government of Alberta in May 2015 (termed "GoA lidar"). The checkpoint locations were locations with GoA lidar where no change of elevation was expected between the acquisition date of the GoA lidar (2007 to 2010) and the acquisition date of the ABMI lidar dataset (2022); specifically, we selected checkpoints at wellpads, intersections of seismic lines, trails, or pipelines.

Both the GoA and ABMI lidar datasets were interpolated into elevation raster files with a spatial resolution of 1 m. The exact elevation of checkpoints was extracted from interpolated elevation rasters. There were two elevation values extracted: GoA lidar and ABMI lidar. Both elevation values for NVA checkpoints were the source of the statistical analysis and the average vertical difference (Zd) was calculated (ASPRS 2015). The average Zd value calculated within three lidar processing subblocks are shown in Table 3. The Zd values for all lidar subblocks were within expected vertical accuracy classes according to ASPRS (2015).

Table 3. Average vertical difference (Zd) values in three subblocks of lidar.

Lidar processing subblock	Number of points	Zd (m)
Block 1	119	0.12
Block 2	90	-0.17
Block 3	82	0.14

After LMS was run and LAS tiles were indexed, we visually inspected point cloud derivatives (bare earth and canopy height models) to detect errors. The most common error types were spikes and data gaps. Spikes were corrected using Global Mapper software to manually reclassify ground points causing the spikes to above ground classification (unclassified). Data gaps were corrected utilizing LAStools to reprocess the tiles with gaps present with updated settings. The final tile dimensions were created based on the Government of Alberta "Specifications and Guidelines" (Provincial Geospatial Centre, 2022).

The lidar data were post-processed to remove noise points and to classify the ground points. We developed a custom R script routine based on the "lidR" algorithm (Roussel et al., 2020; Roussel & Auty, 2023). Using the "lidR" and "LASroads" packages (https://github.com/r-lidar/lidR; https://github.com/Jean-Romain/ALSroads), we derived standardized lidar products for use in vegetation modeling (Table 4).

Table 4. Lidar-derived products used in vegetation modeling workflow.

CCE	Canopy cover estimate
CCE500	Canopy cover estimate for vegetation within 5 m above terrain
CHM	Canopy height model

b. *Lidar-derived structural metrics for linear features*

The lidar-derived values used for the enhanced seismic vegetation inventory (SVI) were canopy cover estimate (CCE), canopy height model (CHM), and canopy cover estimate of vegetation under 5 m (CCE500). The purpose of creating the CCE500 value was to focus on vegetation growing directly on linear corridors and to remove points that might have been returned from adjacent tree canopies taller than 5 m overhanging and shadowing the linear corridor.

To use lidar-derived values, we first compared values determined by field surveys in 2021 and 2022 to calculated lidar values. We also compared canopy cover estimates from stereomodel interpretation to the lidar-derived values.

<u>Comparison of field canopy cover estimates to lidar data</u>

The first comparison was field canopy cover estimates to the lidar-derived values of CCE and CCE500. During field data collection, field crews made notes about canopy cover estimates around established field sites. In the fall of 2021, field crews estimated canopy

cover of vegetation with the potential to grow above 5 m in height and assigned one of the following categories: <25%, 25–70%, and >70%. This estimation took place in an approximately 5 m diameter circle near 37 field sites.

Thirty-seven field sites were established on legacy seismic lines to allow direct comparison of estimated field values of canopy cover to canopy cover estimates derived from lidar point clouds. Only 3 out of the 37 sites (8%) had lidar-derived values outside of the field categories. Thirty-one site locations (84%) had both lidar-derived canopy estimates—CCE and CCE500—within the range of the field category. Another three site locations (8%) had overestimated lidar-derived CCE values due to the presence of adjacent tree canopies overhanging the seismic line corridor, but the CCE500 values were estimated correctly in line with the field category. The results and field photos along with visual representations of CHM and CCE are included in Appendix 1.

During summer 2022, field crews collected very detailed information about the status of vegetation at 47 field sites. The 2022 field protocol was not designed to estimate a single overall canopy cover, as it was in season 2021; instead, field crews estimated canopy covers for vegetation groups separated by height thresholds (>2.5 m, 1–2.5 m, <1 m). Canopy cover for the field site was recalculated as a sum of canopy cover values for vegetation higher than 1 m; these values were then converted into the same categories as data collected in fall 2021 (<25%, 25–70% and >70%) to ensure consistency.

The results of comparison between canopy cover estimates from the 2022 field data and from lidar were very similar to the results from 2021 field data. There were 16 site locations established on legacy seismic lines, and only 3 out of the 16 (19%) had lidar-derived values outside of the field categories. The rest of the site locations (81%) had both CCE and CCE500 estimates in the same canopy cover range.

The results of comparison between canopy cover estimates from the 2022 field data and from lidar were very similar to the results from 2021 field data. There were 16 site locations established on legacy seismic lines, and only 3 out of the 16 (19%) had lidar-derived values outside of the field categories. The rest of the site locations (81%) had both CCE and CCE500 estimates in the same canopy cover range.

The details of the site locations along with 360° photos and snapshots of CCE and CHM are documented in Appendix 1.

Comparison of interpreted canopy cover estimates to lidar data

The second comparison was between stereomodel-interpreted canopy cover estimates and lidar-derived values of CCE and CCE500.

Interpreted values are the interpreter's estimations of observed canopy cover in the stereomodels. As required by project specifications, these values consider only canopy cover of trees on the approved species list. Interpreted estimates should therefore be smaller than values derived from lidar as lidar-derived values do not discriminate between tree species and all vegetation above the height threshold is included in the calculation. This is relevant especially for vegetation within a height of 2 m where a whole mix of shrub species is included in the lidar-derived CCE values but is excluded from the interpreted values. An example comparison of an interpreted canopy cover value (65% of interpreted tree species) against calculated values (79.92% of all species) is in Figure 13.

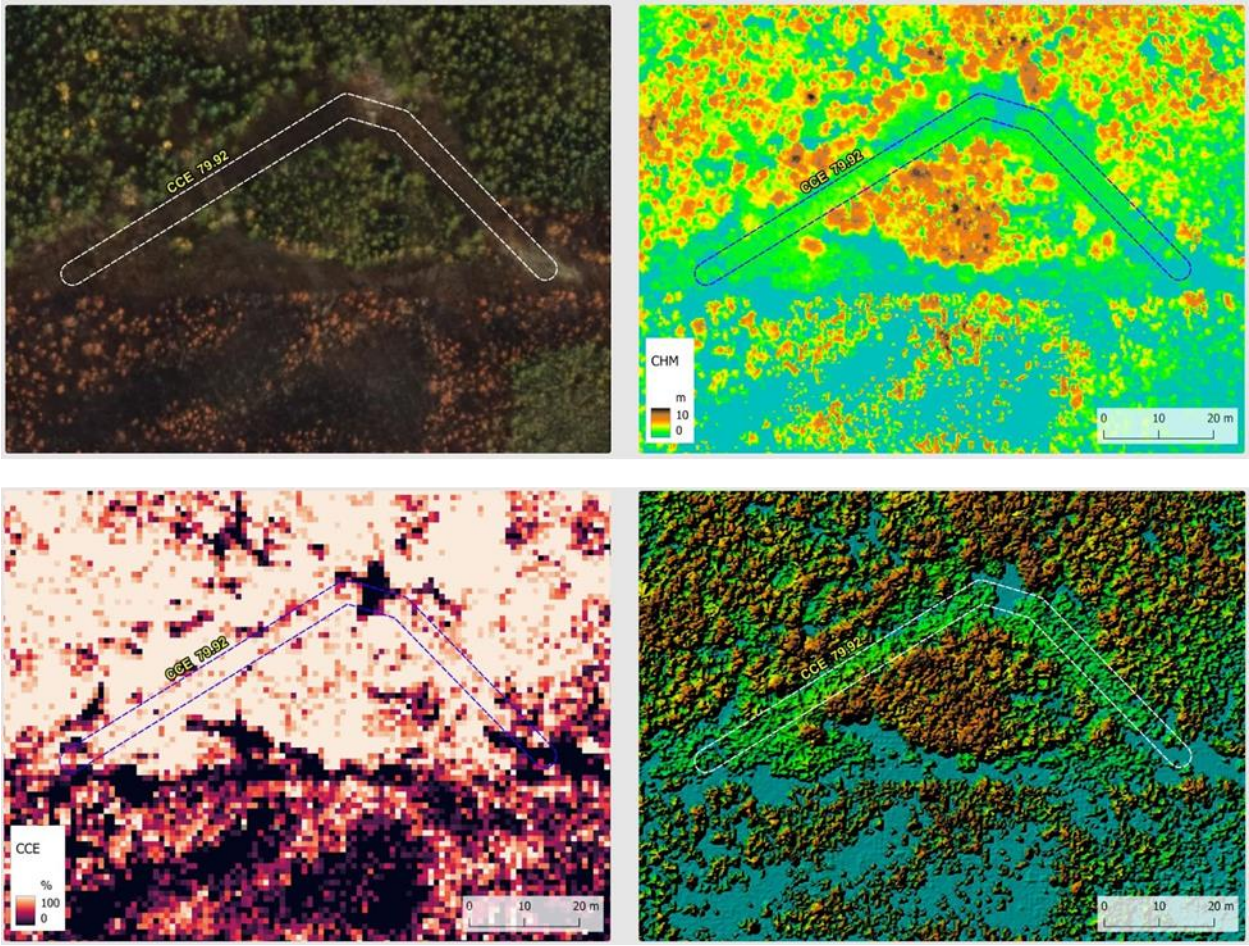

Figure 13. Example of an area with an interpreted canopy cover value of 65% (of accepted tree species). Top left: aerial imagery. Top right: canopy height model layer. Bottom left: canopy cover estimate layer.

As expected, interpreter estimates in the 0–50% range are smaller than lidar-based CCE (Table 5). CCE500 is closer to interpreter estimates. Lidar values align with estimates in the 50–70% range, and are smaller than or similar to interpreted values >70%.

Table 5. Comparison of lidar-derived values for linear features to stereomodel-interpreted canopy cover ranges. Percentages have been rounded to the nearest whole number.

Interpreted canopy cover range	Number of segments	CCE mean [%]	CCE median [%]	CHM mean [m]	CHM median [m]	CCE500 mean [%]	CCE500 median [%]
<25%	453	37	34	1.86	1.03	31	26
25–50%	672	58	60	4.50	3.89	47	47
50–70%	340	63	66	4.16	3.98	56	59
>70%	908	68	73	2.66	2.57	65	70

We also compared lidar-derived metrics of vegetation cover to interpretation-based estimates of vegetation cover to understand the degree to which these two approaches agreed. Interpreters estimated the percent cover of acceptable species along randomly selected seismic line segments (n=51 samples from interpreter 1, n=19 samples from interpreter 2, n=6 of which were interpreted by both). We tested the correlation between these interpretation-based estimates of vegetation cover to lidar-derived estimates of vegetation cover over 50 cm, and estimates of vegetation cover between 50 cm and 5 m using a Pearson's correlation test.

Interpretation-based vegetation cover tended to underestimate vegetation cover relative to lidar-derived metrics (Figure 14). Interpretation-based vegetation cover was correlated with both lidar-derived vegetation cover about 50 cm (CCE; $r^2 = 0.83$, 95% confidence interval: 0.74–0.89, $p < 0.001$) and lidar-derived vegetation cover between 50 cm and 5 m (CCE500; $r^2 = 0.84$, 95% confidence interval: 0.75–0.90, $p < 0.001$).

The results of both canopy cover accuracy analyses—compared to field values and to interpreted values—proved that it is reasonable to consider lidar-derived canopy cover estimate values to represent true canopy cover of the vegetation.

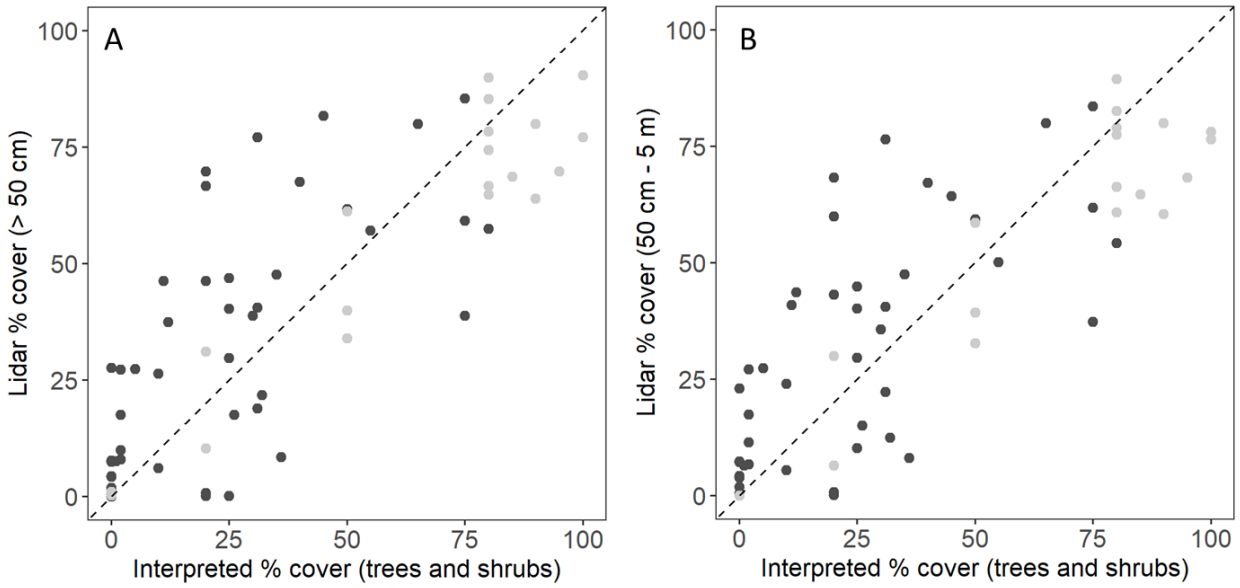

Figure 14. The relationship between interpreted cover of trees and shrubs with lidar-derived vegetation cover above 50 cm (Panel A) and lidar-derived canopy cover between 50 cm and 5 m in height (Panel B). Points are colored by interpreter. The dashed line represents a 1:1 relationship between the two measures of vegetation cover.

Comparison of interpreted canopy height estimates to lidar data

Vegetation heights were also manually interpreted from stereomodels for a subset of seismic lines and trails. Vegetation was assigned one of four height categories: <1 m, 1–2.5 m, 2.5–5 m and >5m.

A direct comparison between manually interpreted values manually and those derived from lidar (i.e., canopy height model values) is not possible: interpreted heights are estimated from the highest point of individual tree crowns only, while CHM values represent multiple values from an entire individual tree crown and also include height values from locations without vegetation. We used the best possible approximation of CHM values to the interpreted values by adjusting CHM values according to canopy cover. This approach removes noise created by including heights of non-vegetated areas within CHM values, but does not correct for the second source of noise, which is averaging multiple height values of individual tree crowns into one mean CHM value.

To compare interpreted vegetation heights to heights derived from lidar, represented as the mean value of CHM (CHMw), we needed to adjust mean CHM values by canopy

coverage values (CCE_mean). The weighted canopy height model value was calculated as follows:

$$CHMw = CHM\_mean/(CCE\_mean/100)$$

The adjusted CHMw values were compared to the interpreted height categories (Table 6).

Table 6. Comparison of stereomodel-interpreted canopy height values for linear features to lidar-derived canopy height models.

Interpreted canopy cover range	Number of interpreted line segments	# of lines with CHMw correct	# of lines with CHMw incorrect	CHMw correct [%]	CHMw incorrect [%]
<25%	29	20	9	69	31
25–50%	127	77	50	61	39
50–70%	263	151	112	57	43
>70%	908	539	368	59	41

It is expected that vegetation canopy cover values would vary depending on landscape conditions. We used ecosite mapping values within the Derived Ecosystem Phase (DEP) dataset to generalize landscape conditions into four site type categories: Upland Dry, Upland and Transitional, Lowland Treed, and Lowland Low Density Treed (Figure 15). We calculated canopy cover estimate values and canopy height estimate values for each site type within the area of DEP dataset overlaid by the lidar dataset within the Richardson project area (Table 7). We were thus able to establish site type canopy cover thresholds based on the average CCE:

- Upland Dry: 38%
- Upland and Transitional: 51%
- Lowland Treed: 51%
- Lowland Low Density Treed: 59%

Table 7. Summary of lidar-derived values for DEP dataset. The number of polygons assessed differs between CCE and CHM due to slight differences in the spatial coverage of the lidar-derived rasters.

Site Type	Number of polygons assessed	CCE mean [%]	Number of polygons assessed	CHM mean [m]
Lowland Low Density Treed	1,995	38	1,978	1.39
Lowland Treed	32,261	51	32,236	2.05
Upland and Transitional	41,208	51	40,374	2.96
Upland Dry	70,684	59	70,456	4.69

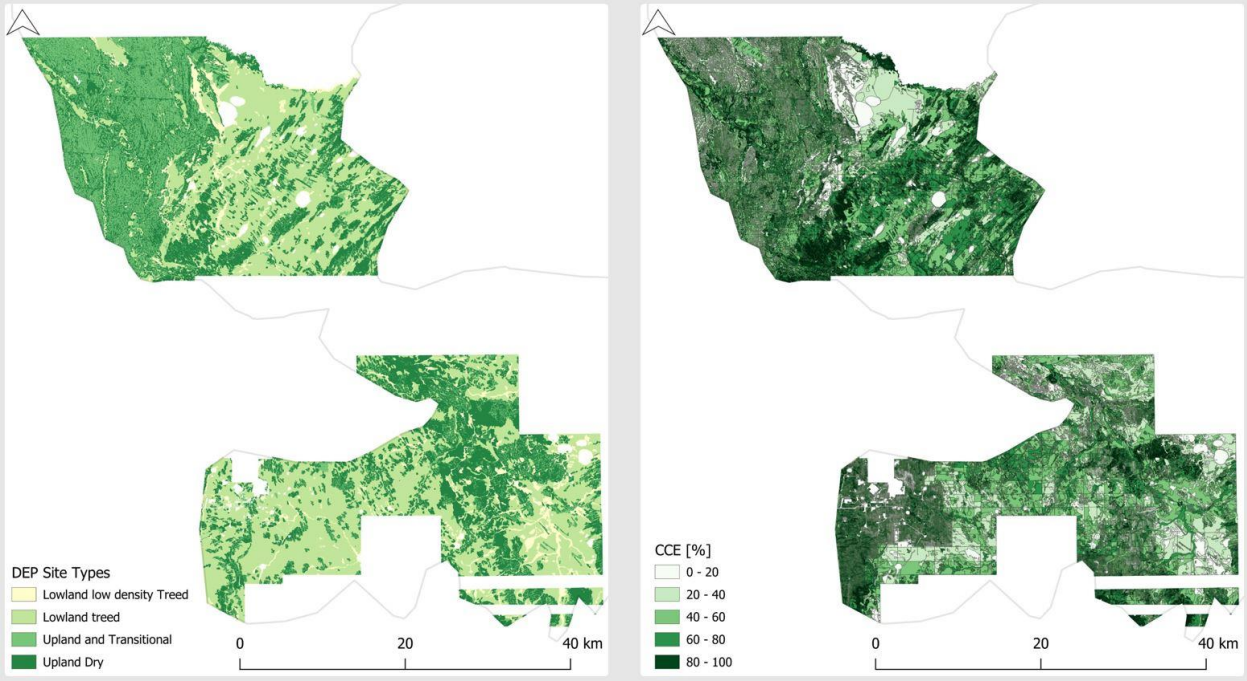

Figure 15. Site types and canopy cover estimates (CCE) for a portion of the Richardson caribou range where DEP data are available. The figure demonstrates how canopy cover thresholds vary between site types and are often below the 70% framework threshold.

4. Indigenous Engagement

Meaningful involvement of and reciprocal relationships with Indigenous communities are an integral part of resource and land management planning. Indigenous communities are key local knowledge holders whose expertise and perspectives are highly valuable in restoration planning, implementation, and monitoring. Our objectives were to invite Indigenous communities to actively participate in project planning and data collection, and to ensure any knowledge and recommendations shared with the ABMI were documented for FRIAA as part of the vegetation inventory.

We worked with the Aboriginal Affairs Advisor at Alberta-Pacific Forest Industries (Al-Pac) to identify Indigenous communities that may have interest in the vegetation inventory project in the Richardson caribou range. As the ABMI did not have previous relationships with the identified communities, Al-Pac initiated contact and introduced the ABMI. The following communities were contacted:

- Athabasca Chipewyan First Nation
- Fort McKay First Nation
- Fort McKay Métis Nation
- Fort McMurray First Nation
- McMurray Métis
- Mikisew Cree First Nation

Of these, Athabasca Chipewyan First Nation, McMurray Métis, and Fort McMurray First Nation did not respond to initial or follow-up requests. Fort McKay First Nation, Fort McKay Métis Nation, and Mikisew Cree First Nation responded with interest. The ABMI then organized initial meetings with office staff for each of these communities to describe the project and answer any questions. All three communities were interested in involving community members in engagement sessions to further explain the project and be involved in its completion.

We successfully held engagement sessions with Fort McKay Métis Nation and Mikisew Cree First Nation. Fort McKay First Nation ultimately did not respond to setting up a session. Each engagement session followed the general agenda below; each community also received a project summary sheet to distribute to community members and a map of the Richardson caribou range. Lastly, we worked with Fort McKay Métis Nation to identify a technician to join 2022 field work; however, due to scheduling conflicts, this did not come to fruition.

The ABMI does not have data sharing agreements to share detailed notes from community engagement sessions, but a summary of important points is as follows:

Fort McKay Métis Nation (FMMN)

One office staff member and five community members attended the engagement session on March 23, 2022. FMMN had previously provided a report to FRIAA on seismic line use by the community in multiple caribou ranges: "Fort McKay Métis Nation Results Memorandum Regarding the Forest Resource Improvement Association of Alberta's (FRIAA) Caribou Habitat Recovery Program". The ABMI read and acknowledged this previous work, especially the identification of important areas in the Richardson caribou range around the Firebag River.

Community members were interested in how old the lines in the Richardson Range were, and they provided information on specific lines that were regrowing well. Fire was brought up as an important factor in how lines were regrowing, and community members suggested that a study be done to understand vegetation trajectory post-fire. Community members noted that many lines are not regrowing well or have snags, which create a maze of sticks and debris. Animals have been observed to hurt themselves (e.g., break their legs) when walking on the lines.

Mikisew Cree First Nation (MCFN)

Two office staff members and six community members attended the engagement session on April 26, 2022. It was noted that a previous study had been done with MCFN and ACFN (Athabasca Chipewyan First Nation) in the Richardson caribou range where interviews were conducted and areas of caribou travel and calving were mapped out. Community members spoke about a fire in the 1990s burning many of the lines that MCFN land users used for travel. As with FMMN, community members described many of the lines as being full of debris and deadfall.

Community members stressed the importance of MCFN involvement in any study on Treaty 8 territory. When consultation happens, MCFN has traplines in the area and would like to be consulted for exclusions. Community members also recommended that FRIAA talk to Treaty 8 Trappers, as well as Métis trappers.

5. Summary of results

Overview of linear feature dataset

Tables 8, 9, and 10 provide breakdowns of the length and number of linear features in different human footprint types as well as by restoration framework action. A complete list of attributes associated with linear features can be found in Appendix 3, while Appendix 4 provides example attribute sets for three adjacent line segments.

The Human Footprint Inventory (HFI) 2021 had over 6,650 km of seismic lines and trails prior to review and correction (Table 8). Following the review process to confirm the existence of linear features in the dataset, identify any missing features in historical datasets, and recentre linear features, there were over 8,300 km in what we termed the Seismic Vegetation Inventory (SVI) dataset (Table 8). We break out linear features by type (legacy seismic, low impact seismic, and trail) and by framework action based on canopy coverage in Table 9. The majority of lines have canopy coverage below the 70% threshold identified in the framework and thus fall into the "treatment" category.

Table 8. Dashboard that summarizes the total length and number of seismic lines included in the Human Footprint Inventory as well as the length and number for each action (treatment, advanced regeneration, exclusion) in the Richardson caribou range.

HFI 2021		Number of segments	Total length of lines (km)	% of total length
Human footprint type	Legacy seismic	3,203	1,798	27.0
	Low impact seismic	34,406	2,929	44.0
	Trail	5,640	1,933	29.0
	Total	43,249	6,659	

Table 9. Dashboard that summarizes the total length and number of seismic lines included in the final Seismic Vegetation Inventory (SVI) dataset in the Richardson caribou range.

SVI		Number of segments	Total length of lines (km)	% of total length
Human footprint type	Legacy seismic	35,171	2,973	35.7
	Low impact seismic	101,402	4,561	54.8
	Trail	7,874	794	9.5
	Total	144,447	8,329	
Framework action category	Advanced regeneration	1,478	75	0.9

SVI		Number of segments	Total length of lines (km)	% of total length
	Treatment	139,107	8,080	97.0
	Exclusion	3,862	174	2.1
	Total	144,447	8,329	

Table 10. Dashboard that summarizes the total length and number of legacy seismic lines, trails, and low impact seismic lines included in the SVI as well as the length and number for each action (treatment, advanced regeneration, exclusion) in the Richardson caribou range.

		Number of segments	Total length of lines (km)	% of total length
Legacy seismic	Advanced regeneration	908	49	1.6
	Treatment	32,343	2,825	95.0
	Exclusion	1,920	99	3.3
	Total	35,171	2,973	
Low impact seismic	Advanced regeneration	415	20	0.4
	Treatment	99,153	4,474	98.1
	Exclusion	1,834	68	1.5
	Total	101,402	4,561	
Trails	Advanced regeneration	155	6	0.8
	Treatment	7,611	781	98.3
	Exclusion	108	7	0.9
	Total	7,874	794	

Summary of lidar-derived values

Overlaying legacy seismic lines and trails with lidar gives us a more fulsome understanding of the status of vegetation on all features. Table 11 shows that the majority (65% of the total length) of linear features assessed have canopy coverage under 25%. Only ~5% have canopy coverage over the framework's recovery threshold of 70%, though lidar estimates may also include non-target species and this may be an overestimate. Linear features with higher canopy cover estimates are concentrated in the central portion of the Richardson range (Figure 16); while lidar coverage was not available for the northern portion, over 75% of linear features were captured in the lidar analysis.

Table 11. Canopy cover estimates for legacy seismic lines and trails in the Richardson caribou range. Estimates were derived from lidar data and validated against interpreted values.

Canopy cover estimate	Number of segments	Total length of lines (km)	% of total length
>=70%	3,057	142	4.9
50% to 70%	3,823	241	8.3
25% to 50%	7,892	624	21.4
<25%	21,826	1,905	65.4
Total	36,598	2,911	

Canopy cover thresholds were established for each of the four site types using lidar data. Table 12 presents an overview of linear features broken out by whether their canopy coverage falls above or below the CCE threshold for their site type. The rightmost column shows that 4-16% of legacy seismic lines and trails (combined) have lidar-based canopy cover estimates above the site type threshold.

Table 12. Summary of length and percent of legacy seismic lines and trails below and above the lidar-based CCE threshold by site type.

Site type	Number of lines	Length [km]	CCE threshold	Number of lines below and above threshold	Length [km]	[%]
Lowland Low Density Treed	1,441	96	≤ 38	1,224	83	86.8
			> 38	217	13	13.2
Lowland Treed	13,205	1,430	≤ 51	12,433	1,370	95.8
			> 51	772	60	4.2
Upland and Transitional	5,406	282	<= 51	4,314	237	84.2
			> 51	1,092	45	15.8
Upland Dry	16,546	1,103	≤ 59	12,976	921	83.5
			> 59	3,570	182	16.5
Total	36,598	2911	≤ Threshold	30,947	2611	89.7
			> Threshold	5,651	300	10.3

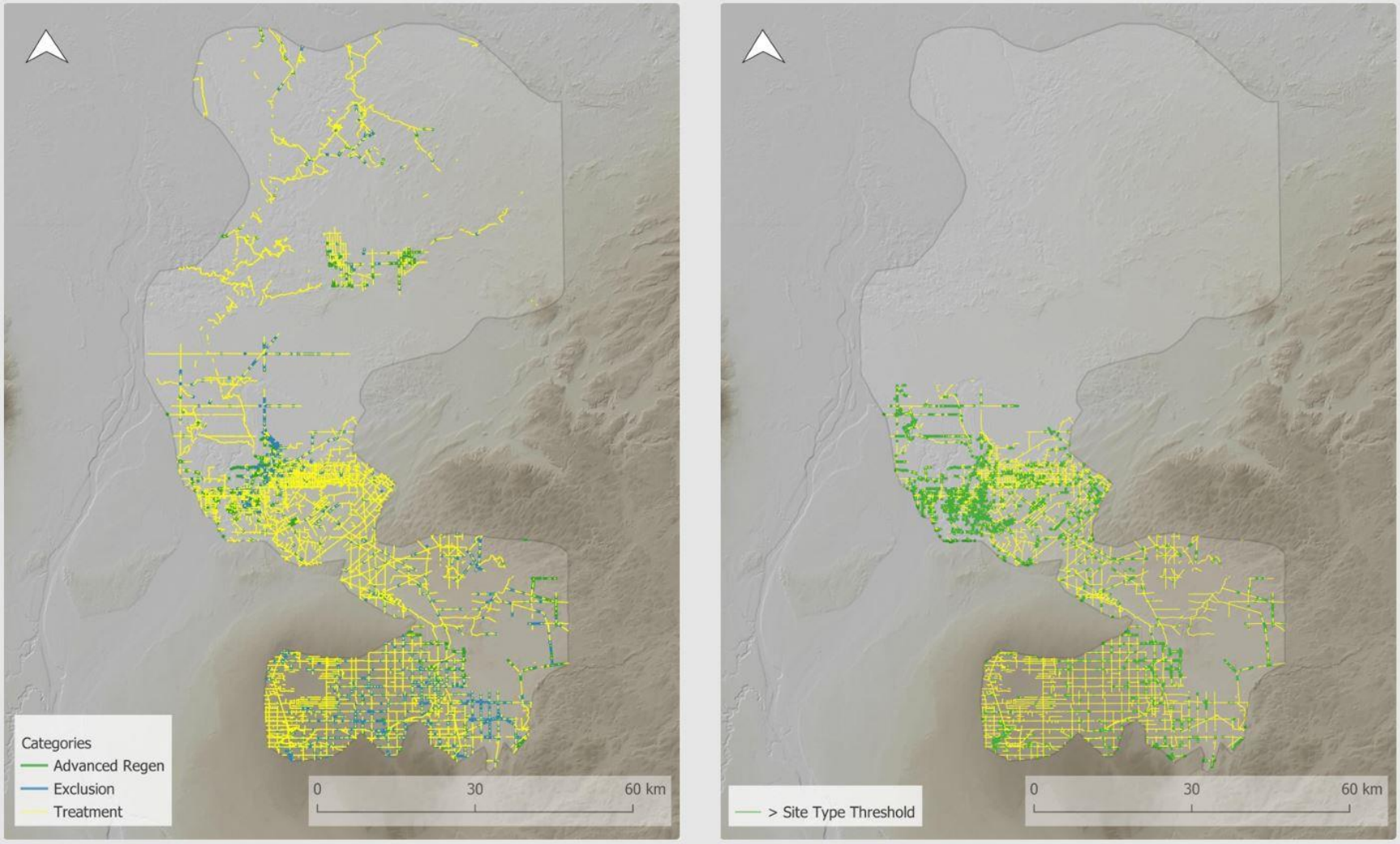

Figure 16. Example of the value of site type-specific regeneration thresholds. The image on the left shows the abundance of lines classified as “treatment” (i.e., below a 70% canopy cover estimate) in the Richardson range. The image on the right shows only legacy seismic lines and trails with canopy cover greater than the average site type threshold derived from lidar. These lines may be further along the trajectory to recovery than a 70% threshold suggests.

This suggests the 70% canopy cover threshold may not be appropriate for all site types, as some undisturbed adjacent forests have much lower canopy cover values. Many linear features may have canopy cover values appropriate for ecosite-specific thresholds and be further along the trajectory to recovery than a comparison to an absolute 70% threshold suggests. The proportion of the range in the “advanced regeneration” category may in fact be much higher. One possible use of this type of information could be to determine the "natural range of variation" in a site type to help inform recovery as measured using CCE and CHM.

Updates to human footprint inventory

Figure 17 demonstrates the value brought to the vegetation inventory by the detailed manual review process of the HFI. Prior to review, there were approximately 6,650 km of linear features mapped in the Richardson caribou range. Following review, over 8,300 km of linear features were mapped, an increase of over 26% or 1,669 km.

Not only were new seismic lines added to the SVI dataset, but feature type categories were also reviewed and updated. There was a significant number of legacy seismic lines attributed as trails in the HFI dataset. These were reviewed and reattributed when needed. The total length of legacy seismic lines in the HFI dataset was 1,780 km and the total number of trails was 1,933 km. The total length of legacy seismic lines in the SVI dataset was 2,973 km and the total number of trails was 794 km.

The sums of both feature types—legacy seismic lines and trails—were relatively close when the HFI and SVI datasets were compared (3,731 km and 3,767 km respectively). This indicates that reattribution was the major driver of differences between the two, rather than adding missing features. The difference in the total length of both feature types between both datasets is smaller than 1%. There was a significant increase in low impact seismic lines between the HFI dataset and SVI dataset (2,929 km and 4,561 km, respectively), an increase of 36% in total length of seismic lines within this category. While the HFI is updated annually, this does not include annual updates to low impact seismic lines. Therefore, both overlooked and new low impact seismic lines are part of the additions in the SVI dataset.

This detailed review enables us to accurately understand the state of vegetation on human footprint in the Richardson caribou range, and track regrowth or lack thereof over time more effectively.

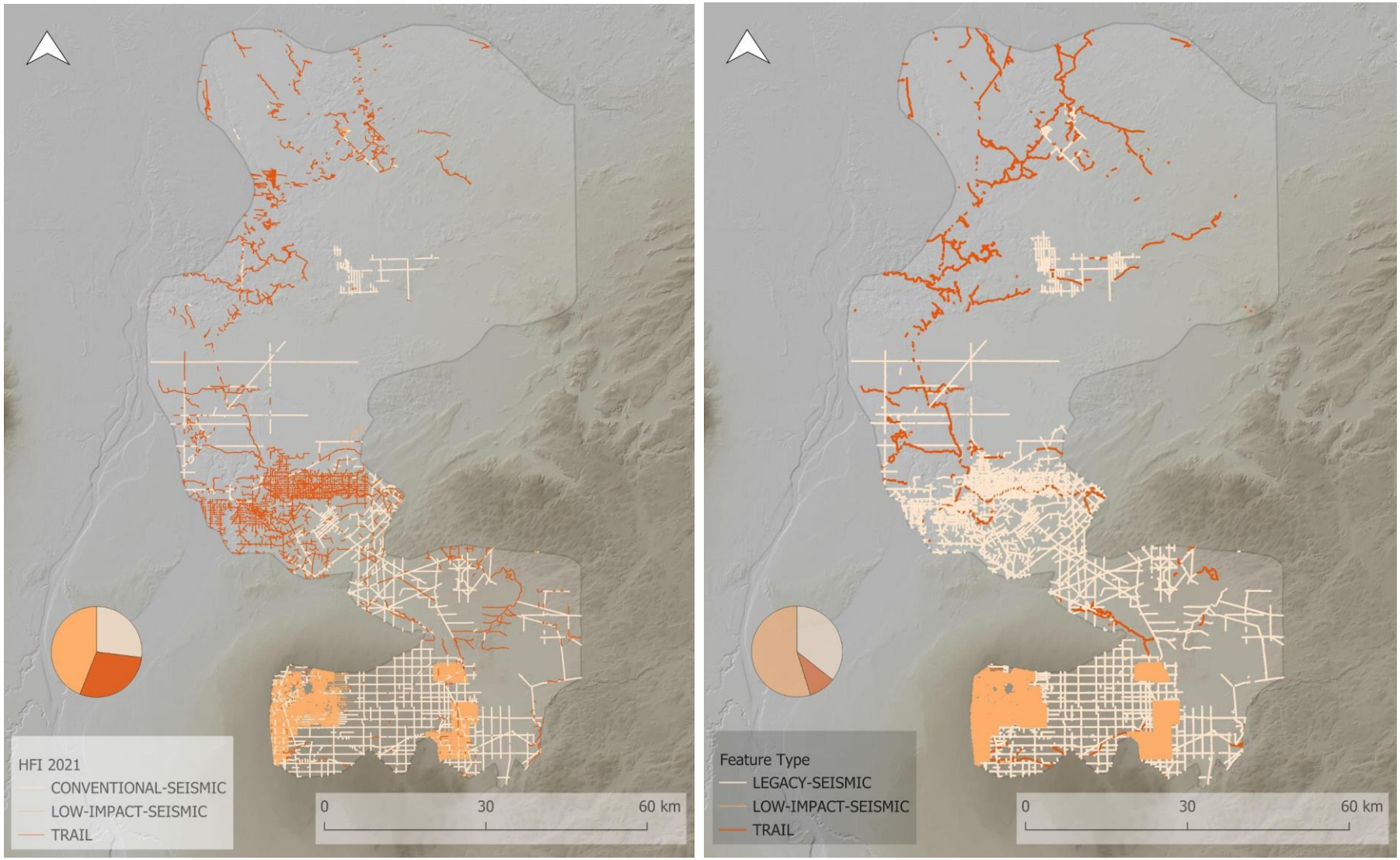

Figure 17. Seismic lines and trails in the Richardson caribou range in the (left) Human Footprint Inventory 2021 and the Seismic Vegetation Inventory (SVI) dataset. The total length of seismic lines and trails is 6,659 km in HFI 2021 and 8,329 km in SVI.

6. Recommendations for future projects

Aerial data collection

There are two aspects of spatial accuracy that must be considered in the interpretation of any features from aerial imagery. The first aspect is absolute (horizontal and vertical) accuracy. The horizontal accuracy of datasets produced using the aerial digital photographs acquired with high-end digital photogrammetric cameras should be within the range of 1.25–1.5x of the pixel size (GSD), the vertical accuracy should be within 2–3x range of the GSD.

The 15 cm imagery provides a horizontal accuracy of approximately 20 cm, and a vertical accuracy of 30 to 45 cm. Therefore, 15 cm imagery can accurately measure vegetation at heights of 60 to 120 cm. This makes 15 cm imagery suitable for an area with recent burns and regeneration, such as the Richardson range.

The second aspect is the ability to recognize and interpret features of interest from the aerial photographs. The objects projected to the aerial photographs through the lens system are generalized into square pixels, with the size of the square's sides equal to the ground sampling distance (GSD). The generic rule of photogrammetry requires at least 3 pixels within the size of the object for the object to be recognizable on aerial imagery, which means the object should be at least 45 cm wide to be recognized on aerial imagery with a spatial resolution of 15 cm. An example of an object that should be recognizable in 15 cm aerial imagery is displayed in Figure 18. Objects that are smaller than the required minimum width (3 x GSD) will be overgeneralized without an ability to recognize them on the aerial imagery. An example is depicted in Figure 19 below.

Figure 18. Example of vegetation that would be recognizable in 15 cm aerial imagery.

Figure 19. Examples of 15 cm (top) and 30 cm (bottom) ground sampling distance (GSD) in an aerial photo compared to the field photo.

The vertical accuracy of the measurements on aerial imagery does depend on the size of the pixel as mentioned above, but it also depends on the target area displayed on the aerial photograph. This is why height measurements of the vegetation (tree, shrubs) are, almost all the time, systematically underestimated, as the top of the tree crown shape is usually narrower than the pixel size. An example of such underestimation is shown in Figure 20.

Figure 20. Example of pixel size at 15 cm (middle) and 30 cm (right) projected vertically at the black spruce sapling. The mass of vegetation large enough to be displayed at the minimum pixel size (15 cm, 30 cm respectively), indicated by the blue marker line, is offset from the measured height by approximately 30 cm (for GSD 15cm) and by 45 cm (for GSD 30 cm).

We also recommend targeting an aerial imagery collection period a few weeks earlier than our collection date to improve the differentiation between trees and shrubs without turning to field data and ecosites.

Alternative datasets

There is great potential for objective, consistent classification of vegetation recovery in the use of lidar for wide-area mapping. Wide-area lidar mapping at sufficient resolutions to capture vegetation at the resolutions required for identifying advanced regeneration as per the Restoration Framework has historically been cost-prohibitive. However, technological advances have increased cost efficiencies for gathering wide-area, high-resolution lidar data. Additionally, analytical advances have increased cost and human resourcing efficiencies for identifying advanced regeneration. These data also offer the opportunity to collect repeated measures in a sub-sampling design in which to evaluate regeneration over time, or to assess treatment effectiveness.

Oblique imagery collected by aerial flyovers provided additional source material to guide interpretation and QAQC interpretations. While these data do not provide quantitative comparisons with interpretations or lidar-based metrics, they are cost-efficient to collect and are value-added to improve interpretation.

Process automation and machine learning

Verifying and correcting the footprint of linear features is a critical step in inventorying vegetation for recovery planning. However, the effort to correct thousands of linear features is not trivial, even with the semi-automated method we employed. Our process was more efficient and spatially accurate than traditional heads-up digitization, as polylines are placed directly on the centres of corridors. Developing further automated methods to delineate and correct the actual footprint of linear features will be a key step for efficient, large-scale vegetation inventories.

Similarly, automating the classification of vegetation is a key next step. Up-to-date, accurate information on the status of vegetation on human footprint across broad spatial scales is critical information needed for evidence-based management of these environments. Remotely sensed data collected across wide areas at high resolutions, such as lidar, have the potential to meet this need, particularly when multiple data sources can be leveraged through machine learning approaches. We demonstrated a first version of a workflow that used machine learning to classify vegetation structure on linear features. Future iterations hold promise to quantify both vegetation composition and structure on human footprint features.

Indigenous engagement

Several community members voiced concern about being engaged too late in the overall process of caribou habitat restoration. Ensure Indigenous communities are engaged prior to the onset of projects to co-develop the objectives and structure. Based on conversations with communities, we recommend that engagement come holistically from the project sponsor and not individual organizations working on specific ranges. This will minimize the duplication of requests to be engaged and share knowledge on a particular topic.

7. Project partners

Several partner organizations supported this program in-kind, including:

- Alberta-Pacific Forest Industries
- Norbord Incorporated
- North West Species at Risk Committee
- Alberta Trappers Association
- Dr. Erin Bayne, Alberta Biodiversity Conservation Chair, University of Alberta
- Dr. Greg McDermid, NSERC Boreal Ecosystem and Recovery Assessment project, University of Calgary
- Suncor Energy
- Cenovus Energy

8. References

ABMI. 2019. Human Footprint Mapping Group Interpretation Guide. ABMI Geospatial Centre.

Applied Geospatial Research Group. 2021. *Forest Line Mapper: A tool for enhanced delineation and attribution of linear disturbances in forests* [Computer software]. Calgary, AB, Canada.

APRS. 2015. ASPRS Positional Accuracy Standards for Digital Geospatial Data. Photogrammetric Engineering & Remote Sensing. 81(3): 1–26.

DeMars C & S Boutin. 2018. Nowhere to hide: effects of linear features on predator-prey dynamics in a large mammal system. Journal of Animal Ecology 87(1): 274–284.

Dickie M, R Serrouya, RS McNay & S Boutin. 2017. Faster and farther: wolf movement on linear features and implications for hunting behaviour. Journal of Applied Ecology 54(1): 253–263.

Dickie M, RS McNay, GD Sutherland, GG Sherman & M Cody. 2021. Multiple lines of evidence for predator and prey responses to caribou habitat restoration. Biological Conservation 256: 109032.

Dickie M, B Hricko, C Hopkinson, V Tran, M Kohler, S Toni, R Serrouya & J Kariyeva. 2023. Applying remote sensing for large-landscape problems: Inventorying and tracking habitat recovery for a broadly distributed Species at Risk. Ecological Solutions and Evidence 4(3): e12254.

Environment and Climate Change Canada. 2020a. Agreement for the Conservation and Recovery of the Woodland Caribou in Alberta. Ottawa, Ontario.

Environment and Climate Change Canada. 2020b. Amended Recovery Strategy for the Woodland Caribou (Rangifer tarandus caribou), Boreal Population, in Canada. https://epe.lac-bac.gc.ca/100/201/301/weekly_acquisitions_list-ef/2021/21-05/publications.gc.ca/collections/collection_2021/eccc/En3-4-140-2020-eng.pdf

Environment Canada. 2012. Recovery Strategy for the Woodland Caribou (Rangifer tarandus caribou), Boreal Population, in Canada. Ottawa, Ontario.

Finnegan L, M Hebblewhite, KE Pigeon. 2023. Whose line is it anyways? Moose (*Alces alces*) response to linear features. Ecosphere 14(8): e4636.

Finnegan L, KE Pigeon, J Cranston, M Hebblewhite, M Musiani, L Neufeld, F Schmiegelow, J Duval & GB Stenhouse. 2018. Natural regeneration on seismic lines influences movement behaviour of wolves and grizzly bears. PLOS ONE 13(4): e0195480.

Finnegan L, R Viejou, D MacNearney, KE Pigeon & GB Stenhouse. 2021. Unravelling the impacts of disturbance type and regeneration on movement of threatened species. Landscape Ecology 36: 2619–2635.

Government of Alberta. 2017. DRAFT Provincial Woodland Caribou Range Plan. Accessed at: https://open.alberta.ca/dataset/932d6c22-a32a-4b4e-a3f5-cb2703c53280/resource/3fc3f63a-0924-44d0-b178-82da34db1f37/download/draft-caribourangeplanandappendices-dec2017.pdf

IPBES. 2019. Global assessment report on biodiversity and ecosystem services of the Intergovernmental Science-Policy Platform on Biodiversity and Ecosystem Services. IPBES secretariat.

McGaughey RJ. 2018. *FUSION/LDV: Software for LiDAR Data Analysis and Visualization* (3.80) [Computer software]. United States Department of Agriculture.

Miller-Rushing AJ, RB Primack, V Devictor, RT Corlett, GS Cumming, R Loyola, B Maas & L Pejchar. 2019. How does habitat fragmentation affect biodiversity? A controversial question at the core of conservation biology. Biological Conservation 232: 271–273.

Nagy-Reis M, M Dickie, P Solymos, SL Gilbert, CA DeMars, R Serrouya & S Boutin. 2020. 'WildLift': An open-source tool to guide decisions for wildlife conservation. Frontiers in Ecology and Evolution 8: 564508.

Provincial Geospatial Centre. 2022. *Airborne LiDAR Data Acquisition - Specifications and Guidelines*. Operational Services, Alberta Environment and Parks.

rapidlasso. 2022. *LAStools* (Computer software). rapidlasso. https://rapidlasso.de

Van Rensen CK, SE Nielsen, B White, T Vinge & VJ Lieffers. 2015. Natural regeneration of forest vegetation on legacy seismic lines in boreal habitats in Alberta's oil sands region. Biological Conservation 184: 127–135.